ST COLUMN TO THE STATE OF THE S

Contents lists available at ScienceDirect

# Computers and Operations Research

journal homepage: www.elsevier.com/locate/cor





# Model and solution method for mean-risk cost-based post-disruption restoration of interdependent critical infrastructure networks

Basem A. Alkhaleel<sup>a</sup>, Haitao Liao<sup>b,\*</sup>, Kelly M. Sullivan<sup>b</sup>

- <sup>a</sup> Department of Industrial Engineering, King Saud University, Riyadh 11421, Saudi Arabia
- <sup>b</sup> Department of Industrial Engineering, University of Arkansas, Fayetteville, AR 72701, USA

#### ARTICLE INFO

#### Keywords: Interdependent infrastructure networks Post-disruption restoration Mixed-integer linear programming

#### ABSTRACT

Critical infrastructure networks (CINs), such as power grids, water distribution systems, and telecommunication networks, are essential for the functioning of society and the economy. As these infrastructure networks are not isolated from each other, their functions are not independent and may be vulnerable to disruptive events (e.g., component failures, terrorist attacks, natural disasters). For decision makers, how to restore the functions of CINs while accounting for interdependencies and various uncertainties becomes a challenging task. In this work, we study the post-disruption restoration problem for a system of interdependent CINs under uncertainty. We propose a two-stage mean-risk stochastic restoration model using mixed-integer linear programming (MILP) with the goal of minimizing the total cost associated with unsatisfied demands, repair tasks, and flow of interdependent infrastructure networks. The restoration model considers the availability of limited time and resources and provides a prioritized list of components to be restored along with assigning and scheduling them to the available network-specific work crews. Additionally, the model features flexible restoration strategies including multicrew assignment for a single component and a multimodal repair setting along with the consideration of full and partial functioning and dependencies between the multi-network components. The proposed model is illustrated using the power and water networks in Shelby County, Tennessee, United States, under two hypothetical earthquake scenarios.

### 1. Introduction

#### 1.1. Background

Modern societies rely on the proper functioning and sustainability of critical infrastructure networks (CINs) such as electric power systems, water supply systems, transportation, and telecommunications (Karakoc et al., 2019). Therefore, maintaining secure and resilient critical infrastructures (CIs) has become one of the most demanding challenges for governments around the globe, especially in the last three decades (White House, 2013; Karagiannis et al., 2017; Humphreys, 2019). For instance, the United States (U.S.) federal planning documents suggest the importance of addressing CI resilience in such a way that reflects its "interconnectedness and interdependency" (White House, 2013). Planning for disruptions to CINs has shifted recently from emphasizing prevention and protection to capturing the CIs' ability to withstand disruptions and quickly recover their functions (Hosseini et al., 2016; Humphreys, 2019). This ability to withstand, adapt to, and recover from disruptions is referred to as

resilience (Barker et al., 2017; Almoghathawi et al., 2019; Humphreys, 2019).

CINs are often vulnerable and subject to natural and/or man-made disruption events (e.g., earthquakes, hurricanes, and malevolent attacks), which could impact the CINs' performance unpredictably and result in severe socioeconomic consequences (Almoghathawi et al., 2019; Alkhaleel et al., 2022). Indeed, such disruptions become inevitable in a modern world featuring growing dynamic and hazardous operating environments (Helbing, 2013). Economically, they have caused huge economic losses around the globe. In the past 50 years, more than 22,500 disasters occurred globally impacting about 8 million people and costing approximately (in 2019 dollar-adjusted value) \$3.7 trillion (CRED, 2021). Annually, only weather-related outages (excluding malevolent attacks and non-weather natural hazards) are estimated to have cost the U.S. economy an inflation-adjusted annual average of \$18 billion up to \$70 billion (Executive Office of the President, 2013; Campbell and Lowry, 2012).

Interdependencies among infrastructure networks have become more frequent and complex due to the increasing trend of globalization

<sup>\*</sup> Corresponding author.

E-mail address: liao@uark.edu (H. Liao).

and technological developments (Rinaldi et al., 2001; Saidi et al., 2018; Karakoc et al., 2019). However, although interdependencies can improve the efficiency of networks functionality, this type of complex coordination often causes them to become more vulnerable to disruptions (e.g., random failures, malevolent attacks, and natural disasters) (Almoghathawi et al., 2021). As a result, a disruption in some components of one of the infrastructure networks could trigger a malfunction in the undisrupted components of other dependent networks, resulting in a series of cascading failures affecting the whole infrastructure network system (Karakoc et al., 2019; Little, 2002; Wallace et al., 2003; Buldyrev et al., 2010; Eusgeld et al., 2011; Danziger et al., 2016; Ouyang, 2014). Although this complex form of interconnectedness of infrastructures was acknowledged two decades ago (Amin, 2002), the related research on interdependent networks only started quite recently as part of resilience engineering applications (Almoghathawi et al., 2019; Buldyrev et al., 2010, 2011; Cavdaroglu et al., 2011; Danziger et al., 2016).

The high vulnerability of infrastructure networks against disruptions and the associated risks of such events have become a critical concern for decision makers, especially with the need to account for the interdependencies through recovery planning to obtain a realistic analysis of their performance (Holden et al., 2013). Moreover, scheduling the restoration processes separately for interdependent critical infrastructure networks (ICINs) without considering their interdependencies could cause misutilization of resources, waste of time and funds, and even might trigger additional inefficiency of distribution systems (Baidya and Sun, 2017). However, functional connectivity among these CIs is not the only dependency that should be taken into account; spatial, cyber, social, and logical interdependencies are other interdependency forms that could impact restoration and recovery planning (Rinaldi et al., 2001; Min et al., 2007; Sharkey et al., 2015).

Recent events such as Hurricane Harvey (Force, 2013) and the 2016 Ecuador earthquake (Meltzer et al., 2019) suggest that not all undesired events can be prevented. In these events and many others, multiple networked systems including the transportation, power, and water networks are impacted (Mendonca et al., 2004; Manuel, 2013; Meltzer et al., 2019). Hence, improving recovery planning actions after disruptions is an essential part of CIs resilience. That is, resilience can be effectively improved by developing optimized plans for promptly restoring the disrupted service after the occurrence of a disruptive event. In planning ICINs restoration, prioritizing components is key in improving the recovery process and system resilience. It is also necessary to consider the practical significant challenges that face recovery actions such as repair times uncertainty and poor access to damaged facilities when developing restoration plans (Karagiannis et al., 2017). To this end, the development of effective restoration strategies and scheduling approaches for CIs post-disruption restoration is typically accomplished through optimization approaches. In the literature, there are numerous studies in the context of post-disruption CI restoration under a mathematical programming framework (Alkhaleel et al., 2022; Nurre and Sharkey, 2014; Vugrin et al., 2014; Fang and Sansavini, 2017; Zhang et al., 2018). Of course, the main goal of such studies is to optimize the scheduling process of restoration tasks in order to accelerate the recovery process and improve the overall resilience (Vugrin et al., 2014).

# 1.2. CIs interdependencies classification

Infrastructure networks are not isolated from each other, but rather they rely on one another in different ways for their proper functioning. Hence, they exhibit interdependency, where a pair of infrastructure networks are said to be interdependent if there is a bidirectional relationship between them through which the state of each infrastructure depends on the state of the other (Rinaldi et al., 2001; Peerenboom et al., 2002). Interdependencies play a critical role in the resilience of CIs by not only contributing to the widespread of failure propagation

(e.g., cascading failures), but also by either facilitating or complicating the entire recovery process (Guidotti et al., 2016). The recovery rate of ICIs components depends on several factors which are often difficult to understand, model, and predict; hence, this uncertainty is reflected on planning the recovery strategy and utilizing related resources (Guidotti et al., 2016; Bruneau et al., 2003; Franchin and Cavalieri, 2015; Sharma et al., 2017). The need to describe the relationships among infrastructure systems, and the corresponding propagation of system disruptions led to the definition of several classifications of the nature of infrastructure interdependencies (e.g., Rinaldi et al., 2001; Lee I.I. et al., 2007; Wallace et al., 2003; Zimmerman, 2001; Zhang and Peeta, 2011). The classification of Rinaldi et al. (2001) is described as a "self-contained classification" that is capable of capturing the different nature of interdependencies (Ouyang, 2014).

The interdependencies between infrastructure networks were classified by Rinaldi et al. (2001) into four categories:

- Physical interdependency: an output from an infrastructure network is an input to another one and vice versa.
- Cyber interdependency: if an infrastructure network depends on information transmitted through an information infrastructure.
- Geographical interdependency: if two infrastructure networks are affected by the same local disruptive event.
- Logical interdependency: all other types of interdependencies (e.g., the social or legal link between two CIs).

Fig. 1 shows the interdependencies between electric power networks and other infrastructure networks. Throughout this article, we focus on the physical interdependencies among different CINs. Note that the physical interdependency defined by Rinaldi et al. (2001) is equivalent to the so-called functional or input interdependency in other classifications (Lee I.I. et al., 2007).

#### 1.3. Related literature

There are several modeling, optimization, and simulation techniques proposed in the literature that consider interdependencies between infrastructure networks (see Ouyang, 2014 for a detailed review). Such techniques can be classified into six categories (Rinaldi, 2004): (i) aggregate supply and demand tools, where infrastructures are linked by their demand for commodities (or services) supplied by other infrastructures (e.g., Enayaty Ahangar et al., 2020), (ii) dynamic simulations, which examines infrastructures operations, the effects of disruptions, and the associated consequences (e.g., Zhang et al., 2016 (iii) agent-based models, where physical components of infrastructures can be modeled as agents allowing the analyses of the operational characteristics, the physical states of infrastructures, and the decisionmaking policies involved with infrastructure operations (e.g., Azucena et al., 2021). (iv) physics-based models, where physical characteristics of CIs can be analyzed with standard engineering techniques such as power flow in electric power grids (e.g., Unsihuay et al., 2007) (v) population mobility models, where this class of models examines the movement of entities (e.g., people following their daily routines) through urban regions (e.g., Casalicchio et al., 2009). (vi) Leontief input-output models, where Leontief's model of economic flows can be applied to CIs studies (Haimes and Jiang, 2001). Throughout this article, the focus will be on the first category with aggregated supply and demand tools.

Post-disruption restoration and recovery problems considering interdependent critical infrastructures (ICIs) have been addressed in the literature through different approaches. Almoghathawi et al. (2021) classifies these approaches into two broad categories: (i) infrastructure-specific approaches, which consider the physics of different infrastructures (e.g., DC power flow model) and hence could be applied on these infrastructure networks only, and (ii) general approaches, which could be applied to any system of interdependent infrastructure networks. Both approaches often fall under the area of combining network design

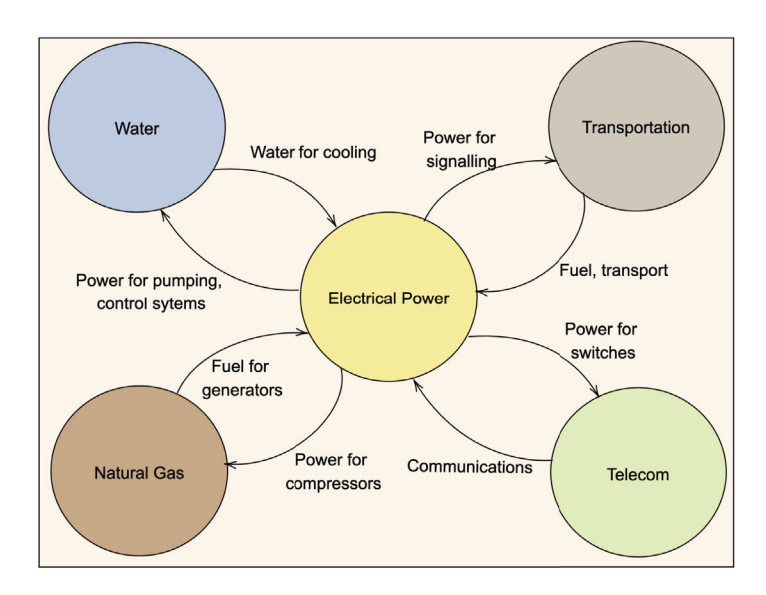


Fig. 1. Examples of electric power infrastructure dependencies. Source: Adapted from Rinaldi et al. (2001).

and scheduling problems following the lead of Nurre et al. (2012) who introduced the integrated network design and scheduling problem (INDS) for restoring a single infrastructure network with the goal of maximizing the cumulative maximum flow over time. Other goals and problem types of post-disruption recovery can be found in the survey article by Çelik (2016) who summarized the work on recovering networks for humanitarian operations and the different problems (decision-making processes) associated with this field of research.

Regarding the infrastructure-specific approaches for interdependent networks restoration, Coffrin et al. (2012) proposed a randomized adaptive decomposition approach to solve the problem of restoring two physically interdependent infrastructure networks, namely power and gas networks. They integrated two network-specific flow models (i.e., a linearized DC flow model for the power network and a maximum flow model for the gas network) using a mixed-integer programming (MIP) approach with the objective of maximizing the weighted sum of interdependent demand over the restoration time horizon. However, their proposed model did not consider different restoration durations for the disrupted components of both networks. Baidya and Sun (2017) presented an optimized restoration strategy with the goal of prioritizing the restoration activities between two physically interdependent infrastructure networks - power and communication networks considering their physical properties. The proposed approach is formulated using MIP with the objective of activating every node in both networks with the minimum number of activation/energization of branches. Tootaghaj et al. (2017) studied the impact of cascading disruption on the physically interdependent power grid and communication network by considering only disruptions in power networks. As a result, they proposed a two-step recovery approach. The first step is to avoid further cascades, for which they formulated the minimum cost flow assignment problem using linear programming with the objective of finding a DC power flow setting that stops the cascading failure at minimum cost. The second step is to provide a recovery schedule, for which they formulated the recovery problem using MIP – with the goal of maximizing the total amount of delivered power over the recovery horizon - and solved the problem using heuristic approaches.

Regarding the general approaches for interdependent infrastructure networks restoration, Lee I.I. et al. (2007) proposed an MIP model for interdependent layer networks accounting for different interdependencies between the infrastructure networks. The objective of the model is to minimize the flow costs along with the costs of unmet demand. Moreover, the model focuses only on determining the set of disrupted

components (i.e., edges) of the interdependent infrastructure networks that need to be recovered to restore the performance of each of the infrastructure networks to its pre-disruption functionality level. Hence, the proposed model does not specify a threshold time at which edges need to be restored nor the assignment of each work crew to restore which disrupted component. On the other hand, Gong et al. (2009) focused only on the scheduling problem of a predetermined set of disrupted components for ICINs with predefined due dates for them. They provided an MIP multi-objective restoration planning model to find the optimal restoration schedule for disrupted components. They proposed a logic-based benders decomposition approach to solve the model, whose objective is to minimize the weighted sum of cost, tardiness, and makespan associated with the restoration process. Cavdaroglu et al. (2011) integrated the two approaches by Lee I.I. et al. (2007) and Gong et al. (2009) by providing an MIP model that: (i) determines the set of disrupted components (i.e., edges) to be restored, (ii) assigns and schedules them to work crews. The model was solved using a suggested heuristic solution method. The objective of the model is to minimize the total cost of flow, unsatisfied demand, and installation and assignment associated with the full restoration of a set of infrastructure networks accounting for their interdependencies. In addition, Holden et al. (2013) proposed an extended network flow approach to simulate the performance of infrastructure networks at a local scale (i.e., community scale) considering the physical interdependency among them. They provided a linear programming optimization model with the goal of finding the optimal performance of the infrastructure networks such that the total cost associated with production, storage, commodity flow, discharge, and shortage (i.e., unsatisfied demand) is minimized. However, the proposed approach by Holden et al. (2013) does not explicitly discuss what is the set of disrupted networks components, their restoration durations, their restoration priorities, and the availability of work crews. Ouyang and Wang (2015) compared the effectiveness of five strategies for joint restoration of interdependent infrastructures and applied a Genetic Algorithm (GA) to generate recovery sequences. Sharkey et al. (2015) studied the restoration of multiple ICINs under a centralized decision-making framework and proposed an MIP model to solve the problem. Additionally, González et al. (2016) proposed an MIP model for optimizing infrastructure systems joint restoration considering geographical and physical interdependencies between multiple CI systems. Di Muro et al. (2016) studied the recovery problem of the system of ICINs in the presence of cascading failures to mitigate its breakdown. They considered the restoration of disrupted network components (i.e., nodes) located at the boundary of the largest connected component in the functional networks. In their study, they tried to reconnect the boundary nodes to the largest connected component considering the probability of recovery that halts the cascade.

In recent years, Zhang et al. (2018) optimized the allocation of restoration resources for a set of physically interdependent infrastructure networks to enhance their resilience. A genetic algorithm was developed to allocate limited resources to interdependent infrastructure networks and to determine the optimal restoration budget following a disruptive event. Mooney et al. (2019) proposed a multiobjective MIP model that integrates a facilities location problem, that determines where resources should be stationed following a disruption, and a recovery scheduling problem to optimize the restoration process of a system of ICIs. Karakoc et al. (2019) proposed a community resilience-driven multi-objective MIP model to schedule the restoration process of disrupted components of a system of ICIs with emphasis on social vulnerability of communities. Almoghathawi et al. (2019) proposed a multi-objective MIP restoration model for systems of interdependent infrastructure networks. Their goal was to find the minimum-cost restoration strategy of a system of interdependent networks that achieves a certain level of resilience. Ghorbani-Renani et al. (2020) proposed a tri-level pre- and post-disruption optimization problem integrating protection, interdiction, and restoration of a system of interdependent networks to improve both vulnerability and recoverability of the system. Garay-Sianca and Pinkley (2021) optimized the restoration of ICIs considering the movement of work crews (machines) through a damaged transportation network being restored by formulating and solving an MIP model.

It is worth pointing out that most studies on post-disruption restoration and recovery of ICINs are based on deterministic assumptions such as complete information on restoration resources and duration of activities (Alkhaleel et al., 2022). However, the restoration of ICINs is complicated by numerous decisions that need to be made in a highly uncertain environment (Fang and Sansavini, 2019). Such uncertainty is linked to several factors including the availability of restoration resources, the time duration for repairing failed components and the accessibility to failed components through the underlying transportation network (Alkhaleel et al., 2022). Moreover, existing optimization approaches do not account for risk measures related to the uncertainty associated with the execution of the optimal plan. Just recently, Alkhaleel et al. (2022) explored integrating risk to resilience-based restoration models; this work showed that it is essential to consider risk-averse decision-making, especially in one-shot applications, which are unrepeatable, such as post-disruption restoration of ICINs. This paper builds upon the previous work by the authors (Alkhaleel et al., 2022); however, here, we extend the previous work to ICINs with an underlying transportation network, explore flexible restoration strategies (i.e., multimode repair and multicrew assignments), and integrate costs of unsatisfied demand (resilience loss equivalent), repair, and flow into the model; with such modifications, we address some of the limitations of the previous work such as: (i) the need to choose between either a risk-neutral approach, which considers the preference criterion in terms of the expectation while comparing the random variables to find the best decisions, or a risk-averse alternative, which incorporates risk measures into the decision making process, to implement (cannot be combined), (ii) assuming binary functional status of each component (either fully functional or disrupted), (iii) preventing concurrent restoration of a single component by multiple crews (a single component can only be restored by one crew), (iv) lack of an economic measure for a developed plan (e.g., using only a resilience measure can cause extra hidden cost in the repair process), (v) unavailability levels of different repair modes for failed components (failed components need to be fully restored).

#### 1.4. Overview and research contribution

In this article, we study the interdependent critical infrastructure networks restoration problem (ICINRP), which seeks to minimize the total cost associated with unsatisfied demand (resilience loss), repair tasks, and network flow by improving the restoration strategy of a system of interdependent networks following the occurrence of a disruptive event considering limited time and resources availability. The goal of this paper is to help decision makers plan for ICIs recovery following the occurrence of a disruptive event not only by improving the speed of system recovery, but by also linking risk and its importance level, assessed by the decision maker, to the restoration plan decisions. Accordingly, a two-stage stochastic optimization model using mixedinteger linear programming was proposed to solve the ICINRP under a mean-risk measure, which combines the risk-neutral and risk-averse approaches into one model. The primary objective of the proposed model is to determine (i) the set of failed components to be restored, (ii) the repair mode for each failed component, (iii) the set of failed components for each crew to restore individually or concurrently, (iv) the baseline restoration sequence across scenarios for each crew in order to minimize the total cost associated with the restoration process (i.e., disruption, repair, and flow costs).

The main contributions of this paper are four-fold. (1) This is the first paper that incorporates a mean-risk approach into ICIs post-disruption restoration models allowing decision makers to choose a risk-averse optimal plan related to a risk importance factor; (2) it explores flexible restoration strategies, and partial functioning and dependencies under uncertainty; (3) it provides an efficient solution approach for solving mean-risk restoration models compared to standard solvers; and (4) the proposed model, solution approach, and flexible restoration strategies are tested using a realistic case study of a system of ICINs in Shelby County, Tennessee (TN), U.S. under two hypothetical earthquake scenarios.

The remainder of this paper is organized as follows. Section 2 presents the background and methodology pertinent to the developed model and summarizes the proposed mathematical formulations. Section 3 provides the solution approach used in this paper. Section 4 presents a case study on the system of ICINs in Shelby County, TN, U.S. to illustrate the use and advantage of the suggested model. Finally, concluding remarks and future research directions are provided in Section 5.

# 2. Methodology and model development

#### 2.1. Risk measure

Before introducing the risk measure approach used in developing the mean-risk two-stage stochastic model, we first define the general form of two-stage stochastic models.

**Definition 2.1.** Given a probability space denoted by  $(\Omega, \mathcal{F}, \mathcal{P})$ , where  $\Omega$  is the sample space,  $\mathcal{F}$  is a  $\sigma$ -algebra on  $\Omega$  and  $\mathcal{P}$  is a probability measure on  $\Omega$ ; for a finite probability space, where  $\Omega = \{\omega_1, \dots, \omega_N\}$  with corresponding probabilities  $\pi_1, \dots, \pi_N$ , the general form of the two-stage stochastic linear programming problem is defined as (Birge and Louveaux, 2011):

$$\min_{\mathbf{x} \in Y} \mathbb{E}(f(\mathbf{x}, \omega)) = \min_{\mathbf{x} \in Y} c^T \mathbf{x} + \mathbb{E}(Q(\mathbf{x}, \xi(\omega)))$$
 (1)

where  $f(x,\omega)=c^Tx+Q(x,\xi(\omega))$  is the cost function of the first-stage problem and:

$$Q\left(\mathbf{x}, \xi^{i}\right) = \min_{\mathbf{y}^{i}} \left\{ \left(\mathbf{q}^{i}\right)^{T} \mathbf{y}^{i} : \mathbf{L}^{i} \mathbf{x} + \mathbf{W}^{i} \mathbf{y}^{i} = \mathbf{h}^{i}, \mathbf{y}^{i} \ge 0 \right\}$$
(2)

is the second-stage problem corresponding to the realization of the random data  $\xi(\omega)$  for event  $\omega_i$ , denoted by  $\xi^i = (q^i, L^i, W^i, h^i)$  where x and y are the vectors of first-stage and second-stage decision variables, respectively.

The general two-stage stochastic optimization model is risk-neutral (i.e., there is no accounting for risk in the objective function). The main goal of such models is to show the effect of incorporating uncertainty compared to deterministic ones. However, although solutions to riskneutral models often perform better than deterministic solutions, both solutions may be subject to poor performance for certain realizations in practice. Such realizations are known as worst-case scenarios in the stochastic optimization literature (Birge and Louveaux, 2011). It is found that under these high-risk scenarios, risk-neutral solutions often perform poorly, especially for CI restoration applications involving both social and economic impacts (Alkhaleel et al., 2022). Given the oneshot nature of CI restoration and its significant socioeconomic impact, it is of interest to consider stochastic models that account for both uncertainty and risk when planning restoration; such models are known as mean-risk models (Noyan, 2012). Mean-risk models are defined as in Definition 2.2:

**Definition 2.2.** For a specific risk measure  $\rho: \mathcal{Z} \to \mathbb{R}$ , where  $\rho$  is a functional and  $\mathcal{Z}$  is a linear space of  $\mathcal{F}$ -measurable functions on the probability space  $(\Omega, \mathcal{F}, \mathcal{P})$ , a mean-risk function is defined as (Noyan, 2012):

$$\min_{\mathbf{x} \in X} \{ \mathbb{E}(f(\mathbf{x}, \omega)) + \zeta \rho(f(\mathbf{x}, \omega)) \}$$
 (3)

where  $\zeta$  is a non-negative trade-off coefficient representing the exchange rate of mean cost for risk.

The change rate of risk  $\zeta$ , hereafter referred to as the risk coefficient, is specified by the decision maker according to the assessment of the associated risk. Toward stating a mean-risk restoration optimization model in Section 2.2, we now summarize the Conditional Value at Risk (CVaR) as the risk measure (Rockafellar and Uryasev, 2000; Krokhmal et al., 2002) and recap some results pertinent to the developed optimization model.

**Definition 2.3.** Let Z denote a *loss* random variable (the term "loss" is used here to indicate that larger values are undesirable) with cumulative distribution function (CDF)  $F(\cdot)$ . For a given risk level  $\alpha \in (0,1]$ , the Value at Risk (VaR) of Z is defined as:

$$VaR_{\alpha}(Z) = \min\{t | F(t) \ge \alpha\} = \min\{t | P(Z \le t) \ge \alpha\}$$
(4)

Thus, for a continuous random variable Z,  $VaR_{\alpha}[Z]$  is the quantile of Z that exceeds the loss with probability  $\alpha$ . The CVaR for Z with risk level  $\alpha \in [0,1]$  is the expected loss given that the loss is at least  $VaR_{\alpha}(Z)$ , i.e.:

$$CVaR_{\alpha}(Z) = \mathbb{E}\left(Z|Z \ge VaR_{\alpha}(Z)\right) \tag{5}$$

It is known that CVaR can also be expressed as the optimal solution to the optimization problem:

$$CVaR_{\alpha}[Z] = \min_{\eta \in \mathbb{R}} \left\{ \eta + \frac{1}{1-\alpha} \mathbb{E}\left[ (Z - \eta)_{+} \right] \right\}$$
 (6)

where  $(a)_+ := \max(a, 0)$  (Rockafellar and Uryasev, 2000). Combining Eqs. (3) and (5), the mean-risk model with a CVaR risk measure can be formulated as:

$$\min_{\alpha \in \mathcal{X}} \left\{ \mathbb{E}(f(\mathbf{x}, \omega)) + \zeta \operatorname{CVaR}_{\alpha}(f(\mathbf{x}, \omega)) \right\}$$
 (7)

Using the result from Eq. (6), Eq. (7) can be rewritten as:

$$\min_{\mathbf{x} \in X, \eta \in \mathbb{R}} \left\{ \mathbb{E}(f(\mathbf{x}, \omega)) + \zeta \left( \eta + \frac{1}{1 - \alpha} \mathbb{E}\left[ (f(\mathbf{x}, \omega)) - \eta_{+} \right] \right) \right\}$$
(8)

#### 2.2. Mean-risk two-stage stochastic program formulation

This section formulates a mean-risk two-stage stochastic program for the ICINRP in which the first-stage schedules the restoration of failed components for each network using multiple network-specific repair crews, chooses the repair mode for each failed component (e.g., perfect or imperfect), and determines the fixed restoration cost of failed components; and the second-stage determines the resulting costs associated with unmet demand and flow for networks under a given realization of the random variables (i.e., repair time for each component and travel times between components). Rather than to optimize explicitly over all random variables, it is common to sample scenarios from their joint distribution. Let  $\Omega$  and  $\Psi$  denote the set of scenarios and networks, respectively. For a given scenario  $\omega \in \Omega$ , let  $ttr^{\psi}_{c\omega}$  denote the time to repair component (either node or arc)  $c \in C'^{\psi}$ . Note that throughout this article we refer to directed (unidirectional) edges as arcs and bidirectional ones as adges. For travel times, let  $tt^{\psi}_{cc}$  denote the travel time from component  $c \in C'^{\psi}$  to component  $c' \in C'^{\psi}$  in the same network. It will also be convenient to define  $\xi(\omega)$  as a vector specifying the realized values of all random variables in scenario  $\omega$ .

An equivalent optimization problem to the mean-risk problem in Eq. (8) can be proposed for a finite probability space  $\Omega = \{\omega_1, \dots, \omega_N\}$  with corresponding probabilities  $\pi_1, \dots, \pi_N$  as shown in Remark 2.1:

**Remark 2.1.** For a finite probability space  $\Omega = \{\omega_1, \dots, \omega_N\}$  with  $|\Omega| = N$  and corresponding probabilities  $\pi_1, \dots, \pi_N$ , an equivalent formulation of the mean-risk problem in Eq. (8):

$$\min_{\mathbf{x} \in X, \eta \in \mathbb{R}} \left\{ \mathbb{E}(f(\mathbf{x}, \omega)) + \zeta \left( \eta + \frac{1}{1 - \alpha} \mathbb{E}\left[ (f(\mathbf{x}, \omega)) - \eta_+ \right] \right) \right\}$$

is the following optimization problem:

$$\min_{\mathbf{x} \in X, \mathbf{y}, \eta \in \mathbb{R}} \quad (1 + \zeta)c^T \mathbf{x} + \sum_{\omega = 1}^{|\Omega|} \pi_{\omega} \left( \mathbf{q}_{\omega} \right)^T \mathbf{y}_{\omega} + \zeta \left( \eta + \frac{1}{1 - \alpha} \sum_{\omega = 1}^{|\Omega|} \pi_{\omega} \nu_{\omega} \right) \quad (9)$$

s.t

$$\mathbf{W}_{\omega}\mathbf{y}_{\omega} = \mathbf{h}_{\omega} - \mathbf{L}_{\omega}\mathbf{x}, \quad \omega = 1, \dots, |\Omega|,$$
 (10)

$$x \in X,\tag{11}$$

$$\mathbf{y}_{\omega} \ge 0, \quad \omega = 1, \dots, |\Omega|$$
 (12)

$$v_{\omega} \ge (q_{\omega})^T y_{\omega} - \eta, \quad \omega = 1, \dots, |\Omega|$$
 (13)

$$\eta \in \mathbb{R}, v_{\omega} \ge 0, \quad \omega = 1, \dots, |\Omega|$$
(14)

The proof of Remark 2.1 can be found in Noyan (2012). This result will be used to formulate the ICINs mean-risk two-stage stochastic programming problem following the notation.

#### 2.2.1. Assumptions

There are several assumptions and considerations for the proposed mean-risk optimization model to solve the ICINRP:

- Each supply node, demand node, and arc in each infrastructure network has a known supply capacity, demand, and flow capacity, respectively.
- Each disrupted component in each infrastructure network can be restored under different possible repair modes (e.g., perfect and imperfect), where each repair mode is related proportionally to the restored capacity of the failed component and the restoration time.
- Imperfect node repair proportionally adjusts a restored node's ability to generate supply or consume demand but assumes nodes are uncapacitated for incoming and outgoing flow (transshipment nodes are only restored in perfect repair mode).
- Each disrupted component in each network can be restored with a different restoration time under each scenario.
- The flow costs through each arc, unmet demand costs, and restoration costs for disrupted components in each infrastructure network are known and fixed.
- Repair times are measured in man-hour units allowing for shorter repair times with a higher number of crews allocated.
- The number of available network-specific work crews for each infrastructure network is known.

#### 2.2.2. Notation

A summary of notation follows. In addition to the notation already defined, the summary defines (i) first-stage binary variables  $x_{cc'k}^{\psi}$  and  $o_{cv}^{\psi}$  in order to encode a restoration plan and choose repair modes for different components (i.e., some disrupted critical components need to be fully repaired to restore the performance of the system while only imperfect repair is needed for other components), (ii) second-stage binary variables  $\kappa^{\psi}_{ckv\omega}(t)$  and  $s^{\psi}_{c\omega}(t)$  in order to resolve the status of each disrupted component and each crew restoration rate for each time period and realized scenario, (iii) second-stage continuous variables  $p^{\psi}_{ck \nu \omega}$  and  $\imath^{\psi}_{ck \nu \omega}(t)$  to mange the assigned restoration task proportion of each component to crews and check the completion of these tasks under each realized scenario, and (iv) flow variables  $f_{iio}^{\psi}(t)$  in order to facilitate determining the maximum weighted flow for each time period and realized scenario. The feasible region of the optimization problem is denoted by X, and the set of decision variables is represented as  $\{x, o, f, u, s, \kappa, st, p, \iota, \eta, v\}.$ 

 $ttr_{co}^{\psi}$ 

ζ

 $\alpha$ 

Parameters & Se	ts
Ψ	Set of infrastructure networks
Y	Set of interdependent nodes $i$ and $i'$ between
	networks $\psi$ and $\psi'$ ( $\psi \neq \psi'$ ) where node $i \in V^{\psi}$
	requires node $i' \in V^{\psi'}$ to be operational
	$((i,\psi)\neq (i',\psi'))$
$G^{\psi}(V^{\psi},A^{\psi})$	Directed graph consisting of nodes $V^{\psi}$ and arcs $A^{\psi}$ for each network $\psi \in \Psi$
$\{V_+^{\psi}, V_*^{\psi}, V^{\psi}\}$	Set of {supply, transshipment, demand} nodes for
('+','*','-')	each network $\psi \in \Psi$
T	The number of time periods in restoration
	planning
$A^{'\psi}$	Set of failed arcs before restoration $(A'^{\psi} \subset A^{\psi})$
	for each network $\psi \in \Psi$
$V^{'\psi}$	Set of failed nodes before restoration $(V'^{\psi} \subset V^{\psi})$
	for each network $\psi \in \Psi$
$C^{\psi}$	Set of all components ( $C^{\psi} = A^{\psi} \cup V^{\psi}$ ) in network
	$\psi \in \Psi$
$C^{'\psi}$	Set of all failed components $(C'^{\psi} = A'^{\psi} \cup V'^{\psi})$ in
	network $\psi \in \Psi$
$K^{\psi}$	Set of repair crews for each network $\psi \in \Psi$
$Y^{\psi}$	Set of repair modes for each network $\psi \in \Psi$
$P_+^{i\psi}$	Supply of node $i \in V_+^{\psi}$ per time period for each
	network $\psi \in \Psi$
$P^{i\psi}$	Demand of node $i \in V_{-}^{\psi}$ per time period for each
	network $\psi \in \Psi$
$P_{ij}^{\psi}$	Flow capacity of arc $(i, j) \in A^{\psi}$ per time period
-	for each network $\psi \in \Psi$
$\chi_y^{\psi}$	Capacity proportion associated with each repair
	mode $y \in Y^{\psi}$
$tt^{\psi}_{cc'\omega}$	Travel time between component $c \in C'^{\psi}$ and
	$c' \in C^{'\psi}$ for each network $\psi$ in scenario $\omega$

Time to repair component  $c \in C'^{\psi}$  for each

Fixed restoration cost for component  $c \in C'^{\psi}$  for

Penalty cost of unmet demand in node  $j \in V^{\psi}_{-}$  for

Unitary flow cost through arc  $(i, j) \in A^{\psi}$  for each

Risk coefficient value representing the risk

weighted importance chosen by the modeler

network  $\psi$  under each scenario  $\omega$ 

Risk level chosen by the modeler

each network  $\psi$ 

each network ψ

network  $\psi$ 

#### **Decision Variables**

$f^{\psi}_{ij\omega}(t)$	Flow on arc $(i, j) \in A^{\psi}$ in time $t \in \{1 T\}$ for
$f^{\psi}_{j\omega}(t)$	each scenario $\omega$ for each network $\psi$ Total flow reaching demand node $j \in V_{-}^{\psi}$ in time $t \in \{1 T\}$ for each scenario $\omega$
$u^{\psi}_{i\omega}(t)$	Amount of unmet demand at node $i \in V^{\psi}$ in time $t \in \{1 T\}$ for each scenario $\omega$
$o_{cy}^{\psi}$	Binary variable indicating whether $(o_{cy}^{\psi} = 1)$ or not $(o_{cy}^{\psi} = 0)$ component $c \in C'^{\psi}$ will be repaired under mode $y \in Y^{\psi}$
$s_{c\omega}^{\psi}(t)$	Binary variable indicating whether $(s_{c\omega}^{\psi} = 1)$ or not $(s_{c\omega}^{\psi} = 0)$ component $c \in C^{\psi}$ is functioning at time $t \in \{0 \dots T\}$
$st^{\psi}_{ck\omega}$	Time at which crew $k \in K^{\psi}$ begins repairing component $c \in C^{'\psi}$ in scenario $\omega$
$p^{\psi}_{cky\omega}$	Continuous variable $\in [0, 1]$ indicating the proportional repair task for each crew $k \in K^{\psi}$ in
	restoring component $c \in C'^{\psi}$ under repair mode $y \in Y^{\psi}$ ; 0 for no contribution and 1 for full restoration by a single crew $k \in K^{\psi}$
$\kappa_{cky\omega}^{\psi}(t)$	Binary variable that equals 1 if component $c \in C'^{\psi}$ is assigned to crew $k \in K^{\psi}$ under repair mode $y \in Y^{\psi}$ and crew $k \in K^{\psi}$ restored the assigned $p_{ck_{Y\psi}}^{\psi}$ by time $t \in \{0 T\}$ ; 0 otherwise
$x_{cc'k}^{\psi}$	Binary variable that equals 1 if crew $k \in K^{\psi}$ repairs component $c \in C'^{\psi}$ before component $c' \in C'^{\psi} \setminus \{c\}$
$\iota^{\psi}_{cky\omega}(t)$	Continuous variable $\in$ [0, 1] indicating whether the proportional restoration task assigned to each crew $k \in K^{\psi}$ for component $c \in C^{'\psi}$ under repair mode $y \in Y^{\psi}$ is accomplished by time $t \in \{1 \dots T\}$
$\eta$ $v_{\omega}$	Auxiliary variable representing the $VaR_{\alpha}$ Continuous variable representing the second-stage costs in scenario $\omega$

The two-stage mean-risk stochastic optimization model for minimizing the expected total cost of the ICINRP follows:

$$\begin{split} \min_{\{x,o,f,u,s,\kappa,st,p,t,\eta,v\} \in X} (1+\zeta) \bigg( \sum_{\psi \in \mathcal{\Psi}} \sum_{y \in Y^{\psi}} c_r^{\psi} o_{cy}^{\psi} \chi_y^{\psi} \bigg) \\ + \sum_{\omega=1}^{|\Omega|} \pi_{\omega} \sum_{\psi \in \mathcal{\Psi}} \sum_{t \in \{1...T\}} \bigg( \sum_{ij \in A^{\psi}} c_f^{\psi} f_{ij\omega}^{\psi}(t) + \sum_{j \in V_{-}^{\psi}} c_d^{\psi} u_{j\omega}^{\psi}(t) \bigg) \\ + \zeta \bigg( \eta + \frac{1}{1-\alpha} \sum_{\omega=1}^{|\Omega|} \pi_{\omega} v_{\omega} \bigg) \end{split} \tag{15}$$

s.t. 
$$\sum_{ij\in A^{\Psi}} f^{\Psi}_{ij\omega}(t) - \sum_{ji\in A^{\Psi}} f^{\Psi}_{ji\omega}(t) \leq P^{i\Psi}_{+},$$
 
$$\forall i \in V^{\Psi}_{+}, \ \forall t \in \{1 \dots T\}, \ \forall \omega \in \Omega, \forall \psi \in \Psi$$
 
$$\sum_{ij\in A^{\Psi}} f^{\Psi}_{ij\omega}(t) - \sum_{ji\in A^{\Psi}} f^{\Psi}_{ji\omega}(t) = 0, \ \forall i \in V^{\Psi}_{*},$$
 (16)

$$\forall t \in \{1 \dots T\}, \ \forall \omega \in \Omega, \forall \psi \in \Psi$$

$$\sum_{ij \in A^{\psi}} f^{\psi}_{ij\omega}(t) - \sum_{ji \in A^{\psi}} f^{\psi}_{ji\omega}(t) - u^{\psi}_{i\omega}(t) = -P^{i\psi}_{-},$$

$$(17)$$

$$\forall i \in V^{\psi}, \ \forall t \in \{1 \dots T\}, \ \forall \omega \in \Omega, \forall \psi \in \Psi$$
 (18)

$$\begin{split} 0 &\leq u_{i\omega}^{\psi}(t) \leq P_{-}^{i\psi}, \ \forall i \in V_{-}^{\psi}, \ \forall t \in \{1 \dots T\}, \ \forall \omega \in \Omega, \forall \psi \in \Psi \\ 0 &\leq f_{ij\omega}^{\psi}(t) \leq s_{ij\omega}^{\psi}(t) P_{ij}^{\psi}, \end{split} \tag{19}$$

$$\forall ij \in A^{\Psi}, \ \forall t \in \{1 \dots T\}, \ \forall \omega \in \Omega, \forall \psi \in \Psi$$

$$0 \le f_{im}^{\Psi}(t) \le s_{im}^{\Psi}(t) P_{ii}^{\Psi}, \ \forall ij \in A^{\Psi}, \forall i \in V^{\Psi},$$

$$(20)$$

$$\forall t \in \{1 \dots T\}, \forall \omega \in \Omega, \forall \psi \in \Psi$$
 (21)

$$0 \le f_{ij\omega}^{\psi}(t) \le s_{i\omega}^{\psi}(t) P_{ij}^{\psi},$$

$$\forall ij \in A^{\Psi}, \forall j \in V^{\Psi}, \forall t \in \{1 \dots T\}, \forall \omega \in \Omega, \forall \psi \in \Psi$$
 
$$0 \leq f^{\Psi}_{ij\omega}(t) \leq \sum_{y \in Y^{\Psi}} o^{\Psi}_{ijy} \chi^{\Psi}_{y} P^{\Psi}_{ij},$$
 (22)

$$0 \le J_{ij\omega}(t) \le \sum_{y \in Y^{\psi}} o_{ijy} \chi_y \, \mathbf{1}_{ij} \,,$$

$$\forall ij \in A'^{\psi}, \ \forall t \in \{1 \dots T\}, \ \forall \omega \in \Omega, \forall \psi \in \Psi$$

$$\sum_{i \in A^{\psi}} f^{\psi}_{ij\omega}(t) - \sum_{i \in A^{\psi}} f^{\psi}_{ji\omega}(t) \le \sum_{v \in Y^{\psi}} o^{\psi}_{iy} \chi^{\psi}_{y} P^{i\psi}_{+},$$
(23)

$$\forall i \in V_{+}^{\Psi} \cap V^{'\Psi}, \forall t \in \{1 \dots T\}, \forall \omega \in \Omega, \forall \psi \in \Psi$$
 (24)

$$\sum_{ij\in A^\psi} f^\psi_{ij\omega}(t) - \sum_{ji\in A^\psi} f^\psi_{ji\omega}(t) \geq - \sum_{y\in Y^\psi} o^\psi_{iy} \chi^\psi_y P^{i\psi}_-,$$

$$\forall i \in V_{-}^{\psi} \cap V^{'\psi}, \forall t \in \{1 \dots T\}, \forall \omega \in \Omega, \forall \psi \in \Psi$$
 (25)

$$s_{-}^{\psi}(0) = 0, \forall c \in C^{'\psi}, \ \forall \omega \in \Omega, \forall \psi \in \Psi$$
 (26)

$$s_{co}^{\psi}(0) = 1, \forall c \in C^{\psi} \setminus C^{'\psi}, \ \forall \omega \in \Omega, \forall \psi \in \Psi$$
 (27)

$$\kappa_{ck \nu \omega}^{\psi}(0) = 0, \ \forall c \in C^{'\psi}, \forall k \in K^{\psi}, \forall y \in Y^{\psi}, \ \forall \omega \in \Omega, \forall \psi \in \Psi$$
 (28)

$$\sum_{y \in Y \notin \mathcal{Y}} o_{cy}^{\psi} \le 1, \forall c \in C^{'\psi}, \forall \psi \in \Psi$$
 (29)

$$o_{cy}^{\psi}t \geq st_{ck\omega}^{\psi} + p_{cky\omega}^{\psi}\chi_{y}^{\psi}ttr_{c\omega}^{\psi} - M(1 - \kappa_{cky\omega}^{\psi}(t)),$$

 $\forall c \in C^{'\psi}, \forall t \in \{1 \dots T\}, \forall k \in K^{\psi},$ 

$$\forall y \in Y^{\psi}, \forall \psi \in \Psi \tag{30}$$

$$\sum_{k \in K^{\psi}} p_{cky\omega}^{\psi} = o_{cy}^{\psi}, \forall c \in C^{'\psi}, \forall y \in Y^{\psi}, \forall \omega \in \Omega, \forall \psi \in \Psi$$
 (31)

$$\begin{split} s_{c\omega}^{\psi}(t) &\leq s_{c\omega}^{\psi}(t+1) \;,\; \forall c \in C^{\psi}, \; \forall t \in \{0 \dots T-1\}, \; \forall \omega \in \varOmega, \forall \psi \in \varPsi \quad \ \ (32) \\ \kappa_{ckwo}^{\psi}(t) &\leq \kappa_{ckwo}^{\psi}(t+1) \;,\; \forall c \in C^{'\psi}, \forall t \in \{0 \dots T-1\}, \end{split}$$

$$\forall k \in K^{\psi}, \forall y \in Y^{\psi}, \ \forall \omega \in \Omega, \forall \psi \in \Psi$$
 (33)

$$st^{\psi}_{ck\omega} + \sum_{y \in Y^{\psi}} p^{\psi}_{cky\omega} \chi^{\psi}_y ttr^{\psi}_{c\omega} + tt^{\psi}_{cc'\omega} \leq st^{\psi}_{c'k\omega} + Mx^{\psi}_{cc'k},$$

 $\forall c, c' \in C'^{\psi} : c \neq c',$ 

$$\forall k \in K^{\psi}, \ \forall \omega \in \Omega, \forall \psi \in \Psi$$
 (34)

$$st^{\psi}_{c'k\omega} + \sum_{y \in Y^{\psi}} p^{\psi}_{c'ky\omega} \chi^{\psi}_y ttr^{\psi}_{c'\omega} + tt^{\psi}_{c'c\omega} \leq st^{\psi}_{ck\omega} + M(1-x^{\psi}_{cc'k}),$$

 $\forall c, c' \in C^{'\psi} : c \neq c',$ 

$$\forall k \in K^{\Psi}, \forall \omega \in \Omega, \forall \psi \in \Psi$$
 (35)

$$st_{ck\omega}^{\Psi} \geq (1 - \sum_{y \in Y^{\Psi}} o_{cy}^{\Psi})T, \forall c \in C^{'\Psi}, \forall k \in K^{\Psi}, \forall \omega \in \Omega, \forall \psi \in \Psi$$
 (36)

$$s_{c\omega}^{\psi}(t) \leq \sum_{k \in K^{\psi}} \sum_{y \in Y^{\psi}} \iota_{cky\omega}^{\psi}(t), \forall c \in C^{'\psi}, \ \forall t \in \{1 \dots T\}, \ \forall \omega \in \Omega, \forall \psi \in \Psi$$

(37)

$$\iota^{\psi}_{cky\omega}(t) \leq \kappa^{\psi}_{cky\omega}(t),$$

$$\begin{split} \forall c \in C^{'\psi}, \forall t \in \{1 \dots T\}, \forall k \in K^{\psi}, \forall y \in Y^{\psi}, \forall \omega \in \Omega, \forall \psi \in \Psi \\ \iota^{\psi}_{cky\omega}(t) \leq p^{\psi}_{cky\omega}, \forall c \in C^{'\psi}, \end{split} \tag{38}$$

$$\forall t \in \{1 \dots T\}, \forall k \in K^{\psi}, \forall y \in Y^{\psi}, \forall \omega \in \Omega, \forall \psi \in \Psi$$
 (39)

$$t^{\psi}_{ckv\omega}(t) \ge p^{\psi}_{ckv\omega} - (1 - \kappa^{\psi}_{ckv\omega}(t)),$$

$$\forall c \in C^{'\psi}, \forall t \in \{1 \dots T\}, \forall k \in K^{\psi}, \forall y \in Y^{\psi}, \forall \omega \in \Omega, \forall \psi \in \Psi$$

$$s_{im}^{\psi}(t) - s_{im}^{\psi'}(t) \le 0,$$

$$(40)$$

$$\forall (i, i') \in Y : (i, \psi) \neq (i', \psi'), \forall t \in \{1 \dots T\}$$

$$\tag{41}$$

$$\sum_{ij\in A^{\psi}} f^{\psi}_{ij\omega}(t) - \sum_{ji\in A^{\psi}} f^{\psi}_{ji\omega}(t) \leq \sum_{y\in Y^{\psi}} o^{\psi}_{i'y} \chi^{\psi}_{y} P^{i\psi}_{+},$$

 $\forall (i, i') \in Y : (i, \psi) \neq (i', \psi'), i \in V_{\perp}^{\psi},$ 

$$\forall t \in \{1 \dots T\}, \forall \omega \in \Omega, \forall \psi \in \Psi$$
 (42)

$$\begin{split} \sum_{ij \in A^{\Psi}} f^{\Psi}_{ij\omega}(t) - \sum_{ji \in A^{\Psi}} f^{\Psi}_{ji\omega}(t) \geq - \sum_{y \in Y^{\Psi}} o^{\Psi}_{i'y} \chi^{\Psi}_{y} P^{i\Psi}_{-}, \\ \forall (i,i') \in Y : (i,\psi) \neq (i',\psi'), \forall i \in V^{\Psi}, \end{split}$$

$$\forall t \in \{1 \dots T\}, \forall \omega \in \Omega, \forall \psi \in \Psi$$
 (43)

$$v_{\omega} \ge \sum_{\psi \in \Psi} \sum_{t \in \{1...T\}} \left( \sum_{ij \in A^{\Psi}} c_f^{\psi} f_{ij\omega}^{\psi}(t) + \sum_{j \in V_{\underline{-}}^{\Psi}} c_d^{\psi} u_{j\omega}^{\psi}(t) \right) - \eta \tag{44}$$

$$x_{cc'k}^{\psi} \in \{0,1\}, \ \forall c \in C^{'\psi}, \forall c' \in C^{'\psi} \setminus \{c\}, \ \forall k \in K^{\psi}, \forall \psi \in \Psi$$
 (45)

$$o_{cy}^{\psi} \in \{0, 1\}, \forall c \in C^{'\psi}, \forall y \in Y^{\psi}, \forall \psi \in \Psi$$

$$\kappa_{ck,vo}^{\psi}(t) \in \{0, 1\},$$

$$(46)$$

$$\forall c \in C^{'\psi}, \ \forall t \in \{0 \dots T\}, \forall k \in K^{\psi}, \forall y \in Y^{\psi}, \forall \omega \in \Omega, \forall \psi \in \Psi$$
 (47)

$$s_{co}^{\psi}(t) \in \{0, 1\}, \forall c \in C^{\psi}, \ \forall t \in \{1 \dots T\}, \forall \omega \in \Omega, \forall \psi \in \Psi$$
 (48)

$$p_{cky\omega}^{\psi} \in [0,1], \forall c \in C^{'\psi}, \forall k \in K^{\psi}, \forall y \in Y^{\psi}, \forall \omega \in \Omega, \forall \psi \in \Psi$$

$$l_{cky\omega}^{\psi}(t) \in [0,1],$$

$$(49)$$

$$\forall c \in C^{'\psi}, \ \forall t \in \{1 \dots T\}, \forall k \in K^{\psi}, \forall y \in Y^{\psi}, \forall \omega \in \Omega, \forall \psi \in \Psi$$
 (50)

$$\eta \in \mathbb{R}$$
(51)

 $v_{\omega} \ge 0, \forall \omega \in \Omega$ (52)

The goal of model (15)-(52) is to determine (i) the set of failed components to be restored, (ii) the repair mode for each failed component, (iv) the set of failed components for each crew to restore individually or concurrently, and (v) the baseline restoration sequence across scenarios for each crew in order to minimize the total cost associated with unsatisfied demand (loss of resilience):  $\sum_{j\in V^{\Psi}}c_{d}^{\Psi}u_{j\omega}^{\Psi}(t)$ , restoration:  $\sum_{y\in Y^{\Psi}}c_{r}^{\Psi}c_{cy}^{\Psi}\chi_{y}^{\Psi}$ , and flow:  $\sum_{ij\in A^{\Psi}}c_{f}^{\Psi}f_{ij\omega}^{\Psi}(t)$  for each network  $\Psi\in\Psi$ . Constraints (16)–(18) are flow balance constraints for each network  $\psi$ . Constraint (19) ensures that the unsatisfied demand  $u_{i\omega}^{\psi}(t)$  for each demand node  $j \in V_{-}^{\psi}$  does not exceed demand  $P_{-}^{i\psi}$  in every time period. Constraints (20)–(22) ensure that the flow on each arc  $(i, j) \in A^{\psi}$  in each time period does not exceed its capacity if the arc and both of its end nodes i, j are functioning (flow is 0 if the arc or one of its nodes is failed). Constraint (23) ensures that the flow on each arc  $(i, j) \in A'^{\psi}$ in each time period does not exceed its capacity associated with the chosen repair mode  $\chi_y^{\psi} P_{ij}^{\psi}$ , where  $\chi_y^{\psi}$  is the percentage of capacity restored for each component under repair mode  $y \in Y^{\psi}$ . Similarly, Constraints (24)-(25) limit the outgoing flow from each failed supply node  $i \in V_{+}^{\psi} \cap V^{'\psi}$  and the incoming flow to each failed demand node  $i \in V^{\psi'} \cap V^{'\psi}$  to the capacities of the nodes associated with the chosen repair modes. Constraints (26) and (27) set the initial state of components to be 0 for failed components and 1 for other components. Similarly, Constraint (28) prevents the completion of failed components restoration by time 0. Constraint (29) prevents assigning more than one repair mode for each failed component. Constraint (30) ensures that crew  $k \in K^{\psi}$  has completed its task of restoring failed component  $c \in C'^{\psi}$  under repair mode  $y \in Y^{\psi}$  the assigned proportion  $p_{ckyo}^{\psi}$  by time  $t \in \{1...T\}$  if and only if the restoration start time added to the task repair time is no more than t. Note that the restoration time of a component as well as its restored capacity depends on the repair mode  $y \in Y^{\psi}$ ; that is, for a repair mode  $y \in Y^{\psi}$  with percentage  $\chi_{v}^{\psi} = \%q$ , both capacity and repair time are reduced by %(1-q). Constraint (31) ensures that restoration assignments for each failed component  $c \in C'^{\psi}$ to all crews do not exceed the restoration task for that component under repair mode  $y \in Y^{\psi}$ . Constraint (32) ensures that components for each network  $\psi$  in  $C^{\prime \psi}$  remain functioning after being restored, and components in  $C^{\psi} \setminus C^{'\psi}$  are functioning for the entire restoration period. Constraint (33) imposes a similar restriction on the  $\kappa_{ck\nu\alpha}^{\psi}(t)$ variables; that is, if crew  $k \in K^{\psi}$  completed the task of repairing component  $c \in C'^{\psi}$  by time period  $t \in \{1 ... T - 1\}$ , where  $\kappa^{\psi}_{ck\nu\alpha}(0) =$  $s_{co}^{\psi}(0)$  at t=0 by Constraint (28), then this task remains completed by time period t + 1. Constraints (34)–(35) manage the restoration scheduling process by ensuring that each crew  $k \in K^{\psi}$  can work on repairing at most one component at a time, according to the schedule specified by the  $x_{cc'k}^{\psi}$ -variables. Relative to Constraints (34)–(35), Constraint (36) prevents scheduling non-selected failed components for

repair throughout the restoration total time T. Defining  $ttr_{ijm}^{\psi \max}$  and  $t_{iji'j'\omega}^{\psi \max}$  as the maximum repair time parameter of any failed component in each network under all scenarios and the maximum travel time parameter between any two failed components in each network under all scenarios,  $M = |A'^{\psi}|(ttr_{ij\omega}^{\psi \max} + tt_{iji'j\omega}^{\psi \max})$  is sufficiently large in Constraint (30) and Constraints (34)–(35). Constraints (37)–(40) ensure the completion of the restoration process for each selected component  $c \in$  $C'^{\psi}$  under repair mode  $y \in Y^{\psi}$  by checking the functional status of each failed component at time  $t \in \{1 ... T\}$  in Constraint (37) based on the completion of each crew  $k \in K^{\psi}$  its assigned task in restoring the failed component in Constraints (38)–(40). Specifically, Constraints (38)–(40) impose that  $t^{\psi}_{cky\omega}(t) = p^{\psi}_{cky\omega} \kappa^{\psi}_{cky\omega}(t)$  and Constraint (37) imposes that component  $c \in C'^{\psi}$  is only functioning at time  $t \in \{1...T\}$  if the cumulative restoration proportion (across all crews) under the selected repair mode  $y \in Y^{\psi}$  is 1. Note how Constraint (37) represents the sum of the products of  $p^{\psi}_{cky\omega}$  and  $\kappa^{\psi}_{cky\omega}(t)$  decision variables via  $t^{\psi}_{cky\omega}(t)$ , and that Constraints (38)–(40) are introduced to linearize the bilinear terms of the sum. Constraints (41)-(43) are the interdependence constraints across networks Y; such constraints ensure that interdependencies between networks given by a set of interdependent nodes across networks Y are respected. In particular, Constraint (41) ensures that a node i in network  $\psi$  that is dependent on node i' in network  $\psi'$ , where  $\psi \neq \psi'$ , cannot function before the functioning of node i'. Similarly, Constraints (42)–(43) restrict the capacity of node i in network  $\psi$  that depends on failed node i' in network  $\psi'$ , where  $\psi \neq \psi'$ , which is restored under repair mode  $y \in Y^{\psi}$  to the proportional capacity  $\chi_{y}^{\psi}$ associated with the chosen repair mode of node i'. Constraint (44) sets  $\eta = VaR_{\alpha}$  based on the second-stage costs associated with unmet demand and flow costs. Constraints (45)–(48) require the  $x_{cc'k}^{\psi}$ -,  $o_{cv'}^{\psi}$ -,  $\kappa_{cky\omega}^{\psi}(t)$ -, and  $s_{c\omega}^{\psi}(t)$  variables to be binary. Constraints (49)–(47) require the  $p_{cky\omega}^{\psi}$  - and  $\iota_{cky\omega}^{\psi}(t)$  variables to be bounded between 0 and 1. Finally, Constraints (51)–(52) require  $\eta$  to be a real number and  $v_{\omega}$  variables to be positive real numbers.

#### 2.2.3. Model variants

Flexible restoration strategies. Compared to a previous work (Alkhaleel et al., 2022), the proposed optimization model (15)–(52), referred to as the standard model hereafter, addresses some limitations (i.e., restricting the restoration of each component to a single crew and allowing only a single maximal repair mode) by considering different flexible recovery strategies including multicrew (MC) and multimode (MM) restoration options. In the former, multiple work crews are allowed to restore a single component of the network  $\psi \in \Psi$  in time  $t \in \{1 ... T\}$ . Compared to a single crew (SC) setting where only one crew is allowed to work on a single component (i.e., each component is restored by at most one crew), it is expected that the MC approach would improve the resilience of the system via minimizing the unsatisfied demand cost, especially when critical components are disrupted. Indeed, changing between an MC setting and an SC setting in the standard model is fairly an easy task. We only need to change the nature of the  $p^{\psi}_{ck_{VO}}$ decision variables from a continuous space  $\in [0, 1]$  for the MC setting to a binary space  $\in \{0, 1\}$  for the SC setting. In the latter strategy, each failed component is restored to a certain level of capacity associated with a repair mode (i.e., for a repair mode with percentage %q, both capacity and repair time are reduced by %(1-q)). Compared to a single mode (SM) repair setting, this strategy can help reduce the repair time of components, especially the ones which do not operate at full capacity before disruption. In Section 4, we compare these restoration strategies and show the added benefit of incorporating such flexible strategies in restoration planning of ICINs under uncertainty.

Partial functioning and interdependency. In addition to the flexible restoration strategies adapted in the standard model, partial functioning and interdependency (PFI) can be implemented by changing the nature of the  $s_{\infty}^{\psi}(t)$  decision variables from binary to continuous variables bounded between 0 and 1. When partial functioning is implemented, components can operate at any capacity in time  $t \in \{1 \dots T\}$ 

below either the full capacity (for a perfect repair mode) or the proportional capacity (for an imperfect repair mode). That is, the binary status assumption of components of the interdependent networks (i.e., either fully functional or failed) is relaxed. Similarly, partial dependence between nodes allows a dependent node to be partially functioning if the node or nodes it depends on are partially functioning as well. However, if the operational nature of the component prevents it from being functional at any partial capacity but instead at only a few possible steps (e.g., a power supply station has four generators and can only function partially depending on the number of working generators at 25%, 50%, 75%, and 100%), then the model can accommodate this change by slight modifications. First, define  $m_c^{\psi}$  and  $m_{c\omega}^{\prime\psi}(t)$  as an integer parameter representing the number of units per component and an integer decision variable representing the number of operational units per component at time  $t \in \{1...T\}$  under scenario  $\omega \in \Omega$ , respectively. Then, by adding a set of constraints of the form:

$$m_c^{\psi} s_{c\omega}^{\psi}(t) \ge m_{c\omega}^{\prime \psi}(t)$$
 (53)

for each component composed of several units and replacing associated  $s_{c\omega}^{\psi}(t)$  decision variables in Constraints (20)–(22) with  $\frac{m_{c\omega}^{\prime\prime}(t)}{m_{c}^{\psi}}$ , we allow stepwise partial functioning linked to the number of operational units. For a system of ICINs that features PFI, it is expected for the system to be more resilient than a counterpart the does not feature PFI due to the reduction in time between the failed state and the first time the disrupted component starts functioning. We compare the PFI setting against the binary status of components in Section 4 to show how PFI affects restoration planning of ICINs under uncertainty.

#### 2.3. ICIs resilience metric

The resilience of a single CI is commonly characterized with respect to a measure of performance (e.g., flow, connectivity, amount of demand satisfied)  $\varphi(t)$  that evolves over time (Henry and Ramirez-Marquez, 2012; Hosseini et al., 2016). In this study, the focus is on the recovery period after disruption, for which a model that optimizes a restoration plan over a finite planning horizon is proposed. Here, we consider the resilience metric proposed by Fang et al. (2016) as the resilience measure of the restoration plans resulting from the standard model. Fang et al. (2016) defines system performance as the maximum amount of weighted flow consumed by the demand nodes. Let weights  $w_j^{\Psi} \in \mathbb{Z}^+$  be assigned to each demand node  $j \in V_j^{\Psi}$  for network  $\psi \in \Psi$ . These weights are incorporated to enable prioritizing certain types of demand nodes (e.g., it is more important to deliver power to a hospital than to a residential household). Formally, the performance for network  $\psi \in \Psi$  is defined as:

$$\varphi^{\Psi}(t) = \sum_{j \in V_{-}^{\Psi}} w_{j}^{\Psi} f_{j}^{\Psi}(t) \tag{54}$$

where  $f_j^{\psi}(t)$  is the total flow reaching demand node j in time period  $t \in \{1, ..., T\}$ .

Based on that, the resilience  $R^{\psi}(T)$  for network  $\psi \in \Psi$  is defined as the cumulative performance restored during the restoration horizon normalized by dividing by the cumulative performance that would be restored over the same horizon if the system could be restored to predisruption performance instantaneously. That is, network resilience is given by Fang et al. (2016):

$$R^{\psi}(T) = \frac{\sum_{t=1}^{t=T} [\sum_{j \in V_{-}^{\psi}} w_{j} f_{j}^{\psi}(t) - \varphi^{\psi}(0)]}{T(\sum_{j \in V_{-}^{\psi}} w_{j} P_{j}^{j\psi} - \varphi^{\psi}(0))}, \quad T \ge 1$$
 (55)

where  $\sum_{j\in V^{\underline{\Psi}}} w_j P_{-}^{j\psi} = \varphi^{\Psi}(t_0)$  denotes the network performance if not affected by the disruption. For one realization  $\omega \in \Omega$ ,  $f_{j\omega}^{\Psi}$  denotes the flow into demand node  $j \in V_{-}^{\Psi}$  in network  $\psi$  under scenario  $\omega \in \Omega$ ;

hence, we can define the resilience  $R^{\psi}(T,\xi(\omega))$  of network  $\psi$  under scenario  $\omega\in\Omega$  as:

$$R^{\psi}(T, \xi(\omega)) = \frac{\sum_{t=1}^{t=T} \left[ \sum_{j \in V_{-}^{\psi}} w_{j}^{\psi} f_{j\omega}^{\psi}(t) - \varphi^{\psi}(0) \right]}{T(\sum_{j \in V_{-}^{\psi}} w_{j}^{\psi} P_{-}^{j\psi} - \varphi^{\psi}(0))}, \quad T \ge 1$$
 (56)

Hence, ICIs system resilience is defined by combining each network resilience in a total resilience term  $R(T, \xi(\omega))$  as follows:

$$R(T, \xi(\omega)) = \sum_{\psi \in \Psi} \gamma^{\psi} R^{\Psi}(T, \xi(\omega))$$
 (57)

where  $\gamma^{\psi}$  is the weight of importance for each network  $\psi$  such that  $\sum_{\psi\in\Psi}\gamma^{\psi}=1.$ 

#### 3. Solution approach

#### 3.1. Scenario generation and reduction

To ensure a representative set of scenarios for the developed optimization model, a maxi-min Latin hypercube sampling (LHS) technique (Wyss and Jorgensen, 1998) is adapted to generate a large set of scenarios  $\Omega$ . Using LHS ensures a fair amount of coverage of each random variable's range, and it has been shown to be advantageous when incorporated within a sample average approximation approach (Alkhaleel et al., 2022; Kleywegt et al., 2002; Chen et al., 2014). However, stochastic optimization models tend to be intractable when the number of generated scenarios is large (Morales et al., 2009). One method often used to overcome this obstacle is to reduce the number of scenarios such that the resulting problem's optimal solution remains close to the solution of the original optimization problem (Fang and Sansavini, 2019; Heitsch and Römisch, 2003; Horejšová et al., 2020). To apply a reduction of scenarios, it is common to select scenarios based upon a probability distance between the original and reduced set of scenarios (Dupačová et al., 2003). The most common probability distance used in stochastic optimization is the Kantorovich distance,  $D_K(\cdot)$ , defined between two probability distributions Q and Q'on  $\Omega$  by the following problem (Rachev, 1991; Dupačová et al., 2003):

$$D_{K}(Q,Q') = \inf_{\theta} \left\{ \int_{\Omega \times \Omega} c(\omega,\omega') \theta(d\omega,d\omega') : \int_{\Omega} \theta(\cdot,d\omega') = Q \right.$$

$$\left. \int_{\Omega} \theta(d\omega,\cdot) = Q' \right\}$$
(58)

Problem (58) is known as the Monge–Kantorovich mass transportation problem (Rachev, 1991), where  $c\left(\omega,\omega'\right)$  is a nonnegative, continuous, and symmetric function, often referred to as cost function. The infimum is taken over all joint probability distributions defined on  $\Omega \times \Omega$  represented by  $\theta\left(\omega,\omega'\right)$  in (58). Note that  $D_K(\cdot)$  can only be properly called Kantorovich distance if function  $c(\cdot)$  is given by a norm. When Q and Q' are finite distributions corresponding to the initial set of scenarios  $\Omega$  and the reduced set of scenarios  $\Omega_s \subseteq \Omega$ , the Kantorovich distance can be determined (see Dupačová et al., 2003 for details) by:

$$D_{K}\left(Q,Q'\right) = \sum_{\omega \in \Omega \setminus \Omega_{s}} \pi_{\omega} \min_{\omega' \in \Omega_{s}} c\left(\omega,\omega'\right)$$
(59)

where  $\pi_\omega$  represents the probability of scenario  $\omega$  in  $\Omega$  (Dupačová et al., 2003). Expression (59) can be used to derive several heuristics for generating reduced scenario sets that are close to an original set (Morales et al., 2009; Dupačová et al., 2003). One well-known algorithm is the fast forward selection algorithm (Heitsch and Römisch, 2003). This algorithm is an iterative greedy process that starts with an empty set; and in each step of the algorithm, a scenario that minimizes the Kantorovich distance between the reduced and original sets is selected from the set of non-selected scenarios ( $\Omega \backslash \Omega_s$ ), where  $\Omega_s$  represents the set of selected scenarios. Then, this scenario is included in the reduced set  $\Omega_s$ . The algorithm terminates either when a pre-specified number of scenarios is found or by reaching a pre-defined Kantorovich distance threshold (Morales et al., 2009).

In the fast forward selection algorithm, as described by Heitsch and Römisch (2003), the distance between two scenarios  $\omega$  and  $\omega'$  is expressed by the function c ( $\omega$ ,  $\omega'$ ) representing the difference between pairs of random vectors. The function c ( $\omega$ ,  $\omega'$ ) can be defined based upon probability metrics (Dupačová et al., 2003), optimal objective function values where first-stage decision variables are fixed (Morales et al., 2009), or the wait-and-see objective value for each scenario, which has been shown to practically outperform the other two methods in restoration modeling (Alkhaleel et al., 2022) and other applications (Bruninx, 2014). Here, we use the objective function value  $z_{\omega}^{WS}$  of the wait-and-see solution (WS) for each scenario  $\omega \in \Omega$  (i.e., the objective function resulting from solving model (15)–(52) when it is populated with  $\omega$  as its only scenario) to define  $c(\cdot, \cdot)$  as follows:

$$c(\omega, \omega') = \left| z_{\omega}^{WS} - z_{\omega'}^{WS} \right| \tag{60}$$

The resulting fast forward selection algorithm can be found in Alkhaleel et al. (2022).

#### 3.2. Decomposition algorithm

Decomposition algorithms are often used for solving continuous and mixed-integer large-scale two-stage and multi-stage optimization problems (Escudero et al., 2017; Rahmaniani et al., 2017). One of those types of algorithms is the well-known Benders decomposition (Benders, 1962), which is commonly used in the stochastic optimization literature to solve the scenario-based resulting mixed-integer linear programs (MILPs). Benders decomposition is a variable partitioning technique in which a restricted master problem is solved considering only the complicating variables of the problem. Such variables are temporarily fixed, and the resulting individual or multiple subproblems are solved to identify cuts to be added to the restricted master problem. In this context, the mean-risk model separates into one linear program per scenario  $\omega$ —forming the subproblem (SP)—in the reduced scenario set  $\Omega_s$  after fixing the binary  $\sigma_{cv}^{\psi}$ - and  $s_{c\omega}^{\psi}(t)$ -variables.

Formally, for each scenario  $\omega \in \Omega_s$ , let  $\overline{z}_\omega$  denote a fixed assignment of values to all o- and s-variables corresponding to the index  $\omega$ . The resulting SP for scenario  $\omega \in \Omega_s$  is the linear program:

$$SP(\overline{z}_{\omega}): \min \sum_{\psi \in \Psi} \sum_{t \in \{1...T\}} \left( \sum_{ij \in A^{\psi}} c_f^{\psi} f_{ij\omega}^{\psi}(t) + \sum_{i \in V_{-}^{\underline{\psi}}} c_d^{\psi} u_{j\omega}^{\psi}(t) \right)$$
(61)

s.t. (16)–(25) and (42)–(43) for scenario 
$$\omega$$
 (62)

Because  $SP(\overline{z}_{\omega})$  is a linear program in which  $\overline{z}_{\omega}$  appears only in the constraints, the dual of  $SP(\overline{z}_{\omega})$  can be formulated as a linear program of the form:

$$DSP(\overline{z}_{\omega}): \max \left(b_{\omega} - B_{\omega}\overline{z}_{\omega}\right) d_{\omega}$$
 (63)

s.t. 
$$d_{\omega} \in \mathcal{D}$$
 (64)

where  $\boldsymbol{b}_{\omega}$  is the right-hand side vector of (62),  $\boldsymbol{B}_{\omega}$  is the left-hand side coefficient matrix of (62),  $\boldsymbol{d}_{\omega}$  is the dual variable vector corresponding to constraint (62), and  $\mathcal{D}$  represents the dual feasible region. Let  $\mathcal{D}_p$  and  $\mathcal{D}_r$  respectively denote the extreme points and extreme rays of  $\mathcal{D}$ , and let  $\mathcal{D}_p^{on} \subseteq \mathcal{D}_p$  and  $\mathcal{D}_r^{on} \subseteq \mathcal{D}_r$  respectively denote a subset of the extreme points and extreme rays produced prior to iteration n of Benders decomposition. Using the optimal solutions of DSP( $\bar{z}_{\omega}^n$ ) from previous iterations  $\{0 \dots n-1\}$ , the restricted master problem (RMP) for iteration n can be formulated as:

$$\min (1+\zeta) \left( \sum_{\psi \in \Psi} \sum_{y \in Y^{\psi}} c_r^{\psi} o_{cy}^{\psi} \chi_y^{\psi} \right) + \lambda_1 + \zeta \lambda_2$$
 (65)

s.t. 
$$\lambda_1 \ge \sum_{\omega=1}^{|\Omega_s|} \pi_{\omega} \left( \boldsymbol{b}_{\omega} - \boldsymbol{B}_{\omega} \boldsymbol{z}_{\omega} \right) \overline{\boldsymbol{d}}_{\omega}^i, i = 0 \dots n - 1$$
 (66)

$$\lambda_2 \ge \eta^i + \frac{1}{1 - \alpha} \sum_{\omega=1}^{|\Omega_s|} \pi_\omega v_\omega^i, \ i = 0 \dots n - 1$$
 (67)

$$v_{\omega}^{i} \ge (\boldsymbol{b}_{\omega} - \boldsymbol{B}_{\omega} \boldsymbol{z}_{\omega}) \, \overline{\boldsymbol{d}}_{\omega}^{i} - \eta^{i}, \forall \omega \in \Omega_{s}, \ i = 0 \dots n - 1$$
 (68)

$$0 \ge \left( \boldsymbol{b}_{\omega} - \boldsymbol{B}_{\omega} \boldsymbol{z}_{\omega} \right) \overline{\boldsymbol{d}}_{\omega}^{i}, \forall \omega \in \Omega_{s}, \ i = 0 \dots n - 1$$
constraints (26)–(41) and (45)–(52)

where i denotes the ith iteration cut generated prior to the current iteration related to  $\mathcal{D}_{n}^{\omega n}$  for Constraints (66)–(67) and  $\mathcal{D}_{r}^{\omega n}$  for Constraint (69). Note that Constraint (68) is equivalent to Constraint (44) in the standard model. Constraints (66)-(67) and (69) are respectively known as optimality cuts and feasibility cuts.

In the proposed Benders algorithm (Algorithm 1), the first step is to set the upper bound, lower bound, and iteration counter at  $\infty$ , 0 and 0, respectively. In iteration n, RMP is solved first to obtain an optimal solution  $\bar{z}^n$ . Letting  $\bar{z}^n_{\omega}$  denote the partial solution associated with the o- and s-variables corresponding to the index  $\omega$ , DSP( $\bar{z}_{\omega}^{n}$ ) is solved (note that since the linear program in (61)-(62) and so its dual (63)–(64) are scenario indexed, they can be solved in parallel providing multicuts), yielding either an extreme point  $\overline{d}_{\omega} \in \mathcal{D}_p$  (if the model is solved to optimality) or an extreme ray  $\overline{\boldsymbol{d}}_{\omega} \in \mathcal{D}_{p}$  (if the model is concluded to be unbounded). In the former case,  $\overline{d}_{\omega}^{r}$  is added to  $\mathcal{D}_{n}^{\omega n}$ (i.e.,  $\mathcal{D}_p^{\omega,n+1} \leftarrow \mathcal{D}_p^{\omega n} \cup \{\overline{\boldsymbol{d}}_\omega\}$  and  $\mathcal{D}_r^{\omega,n+1} \leftarrow \mathcal{D}_r^{\omega n}$ ), resulting in a new optimality cut; otherwise,  $\overline{\boldsymbol{d}}_\omega$  is added to  $\mathcal{D}_r^{\omega n}$  (i.e.,  $\mathcal{D}_p^{\omega,n+1} \leftarrow \mathcal{D}_p^{\omega n}$  and  $\mathcal{D}_r^{\omega,n+1} \leftarrow \mathcal{D}_p^{\omega n} \cup \{\overline{\boldsymbol{d}}_\omega\}$ ), yielding a new feasibility cut. The RMP objective provides a lower bound to the optimal solution of the original problem (15)–(52); furthermore, the dual subproblem DSP( $\bar{z}_{\omega}$ ) always has an optimal solution due to the feasibility and boundedness of the  $SP(\overline{z}_{\omega})$ , which can be easily proven by showing that the restricting the flow under each scenario to 0 provides a feasible solution and that the flow is bounded by the capacities of the demand nodes (see Alkhaleel et al., 2022 for details). This remark shows that feasibility cuts are not needed in the decomposition procedure; therefore, only optimality cuts are generated and added to the RMP in each iteration (as shown in Algorithm 1) and the convergence of the algorithm is accelerated. The optimality gap for this algorithm can be estimated using the upper and lower bounds found at each step. That is, the optimality gap is calculated as Gap(%) =  $\frac{UB-LB}{UB} = \frac{\hat{\mu} + \lambda^* - (\hat{\mu} + \overline{\lambda})}{\hat{\mu} + \lambda^*} = \frac{\lambda^* - \overline{\lambda}}{\hat{\mu} + \lambda^*}$ .

#### 4. Case study

In this section, we test the proposed mean-risk optimization model and solution algorithm, and explore the introduced flexible restoration strategies and PFI using a realistic, well-known case in the literature on the system of ICINs in Shelby County, TN, U.S. This county, containing the city of Memphis, is continually under earthquake hazard due to its proximity to the New Madrid Seismic Zone (NMSZ) (González et al., 2016; Almoghathawi et al., 2021). Here, we consider two cases similar to the hypothetical earthquake scenarios with magnitudes  $M_w \in \{6,7\}$ presented by González et al. (2016).

#### 4.1. System description

The system of interdependent networks considered in this study consists of two ICINs located in Shelby County, TN: power and water as depicted in Fig. 2 (González et al., 2016). The system of networks contains 256 network components divided into 109 nodes and 147 edges. The power network is composed of 60 nodes and 76 edges, and the water network is composed of 49 nodes and 71 edges. For the water system, storage tanks and large pumps are modeled as generation (supply) nodes and pipe intersections are modeled as water distribution (demand) nodes (Kim et al., 2007). Moreover, gate stations are modeled as power generation (supply) nodes and substations are modeled as power distribution (demand) nodes for the power network. The actual system, managed by the Memphis Light, Gas, and Water (MLGW), is a heterogeneous mix of unidirectional arcs and bidirectional edges (Kim et al., 2007). However, it can be modeled either as Algorithm 1: Benders decomposition algorithm

**Step 0:**  $UB \leftarrow \infty, LB \leftarrow 0$ , iteration counter n = 0

Step 1: Solve the RMP (65)-(69) to obtain its optimal solution  $(\overline{z}, \overline{\lambda}_1, \overline{\lambda}_2)$  and let  $\hat{\mu}$  be the optimal first-stage cost and

Solve the DSP( $\overline{z}_{\omega}$ ) to obtain its optimal solution  $\overline{d}_{\omega}^{n}$  and objective value  $(\boldsymbol{b}_{\omega} - \boldsymbol{B}_{\omega} \overline{\boldsymbol{z}}_{\omega}) \overline{\boldsymbol{d}}_{\omega}^{n}$ 

**Step 3:** Find the  $\alpha$ -quantile  $\overline{\eta}$  across all DSP( $\overline{z}_{\omega}$ ) and associated  $\text{CVaR}_{\alpha}$  function, denoted as  $\hat{\lambda}_2$ :  $\hat{\lambda}_{2} = \overline{\eta} + \frac{1}{1-\alpha} \left( \sum_{\omega=1}^{|\Omega_{s}|} \pi_{\omega} \left[ (\boldsymbol{b}_{\omega} - \boldsymbol{B}_{\omega} \overline{\boldsymbol{z}}_{\omega}) \ \overline{\boldsymbol{d}}_{\omega}^{n} - \overline{\eta} \right]_{+} \right)$ 

Step 4: Let  $(\eta^n, v_\omega^n) = (\overline{\eta}, [(b_\omega - B_\omega \overline{z}_\omega) \overline{d}_\omega^n - \overline{\eta}]_+)$ Step 5: Find the mean-risk function value, denoted as  $\lambda^*$ , of the current recourse cost solution:

$$\begin{split} \lambda^* &= \sum_{\omega=1}^{|\Omega_s|} \pi_\omega \left( \boldsymbol{b}_\omega - \boldsymbol{B}_\omega \overline{\boldsymbol{z}}_\omega \right) \overline{\boldsymbol{d}}_\omega^n + \zeta \ \hat{\lambda}_2 \\ U\boldsymbol{B} &\leftarrow \min\{U\boldsymbol{B}, \hat{\mu} + \lambda^*\} \end{split}$$

**Step 6:** If  $UB - LB \le \epsilon$ :  $\triangleright \epsilon$  is a predefined tolerance Stop and report solution Else:

> (a) Add optimality cuts of the form:  $\lambda_{1} \geq \sum_{\omega \in \Omega_{s}} \pi_{\omega} \left( \boldsymbol{b}_{\omega} - \boldsymbol{B}_{\omega} \boldsymbol{z}_{\omega} \right) \overline{\boldsymbol{d}}_{\omega}^{n}$   $\lambda_{2} \geq \eta^{n} + \frac{1}{1-\alpha} \sum_{\omega=1}^{|\Omega_{s}|} \pi_{\omega} v_{\omega}^{n} \text{ to the RMP}$ (b) Add a total number of  $|\Omega_{s}|$  Benders optimality cuts

 $v_{\omega}^{n} \geq \left( \boldsymbol{b}_{\omega} - \boldsymbol{B}_{\omega} \boldsymbol{z}_{\omega} \right) \overline{\boldsymbol{d}}_{\omega}^{n} - \eta^{n}, \forall \omega \in \Omega_{s} \text{ to the RMP}$  (c)  $n \leftarrow n+1$  and go to Step 1

End If

a system of directed networks or undirected networks using network flow approaches (Ahuja et al., 1993). In this study, we model the utility networks as directed networks where directed arcs are modeled to send flow in one direction and bidirectional edges are modeled as two directed arcs. Note that the flow in power networks is governed by physics-based power flow constraints that can be added to the model with slight modifications (Alkhaleel et al., 2022). However, since the relevant information on power reactance values here is not available, such constraints have been omitted in this work (Almoghathawi et al., 2021; Morshedlou et al., 2018). Additionally, the functional dependency considered in this study is unidirectional (i.e., only the water network depends on the power network) where each water generation node is dependent on at least one power distribution node. Flow units per hour are in MWh for the power network and million gallons hourly  $(MGh)\times 10^2$  or 10kGh for the water network.

# 4.2. Uncertainty representation

The proposed model assumes that the time to repair each component and the travel time between failed components are uncertain, but the remaining parameters are deterministic. The remainder of this section summarizes the assumed probability distributions for the uncertain parameters.

Let  $C' \subseteq C$  denote the set of disrupted components, and  $ttr_c$  denote the time to repair of component  $c \in C'^{\psi}$ . We assume  $ttr_c$  has a Weibull distribution - commonly used to model activity times (Abdelkader, 2004) – with scale parameter  $v_c$  and shape parameter  $\beta_c$ . The probability density function of ttr<sub>c</sub> is given by:

$$h(t, \beta_c, \nu_c) = \frac{\beta_c}{\nu_c} \left(\frac{t}{\nu_c}\right)^{\beta_c - 1} e^{-\left(\frac{t}{\nu_c}\right)^{\beta_c}}, \ t \ge 0$$
 (70)

As for travel times, for  $c \in C'^{\psi}$  and  $c' \in C'^{\psi}$ , let  $t_{cc'}^{\psi}$  denote the travel time between components c and c' in network  $\psi$ . We derive a

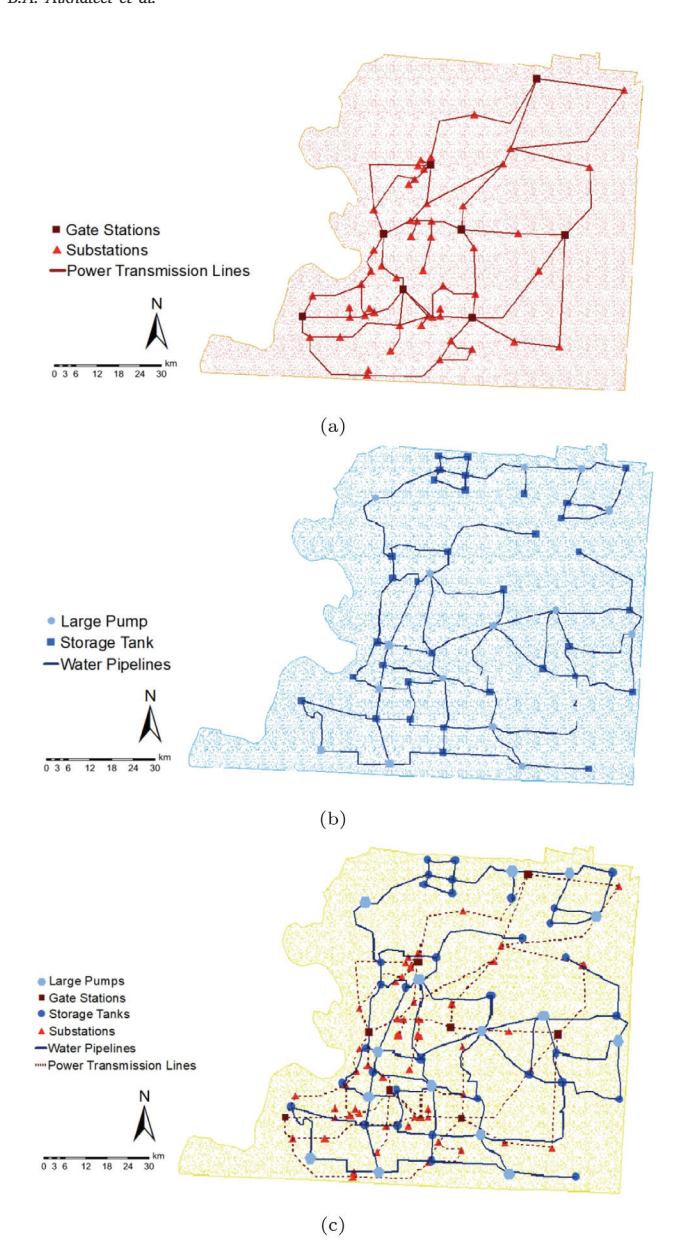


**Fig. 2.** Graphical representations of the (a) power, (b) water, and (c) combined water and power networks in Shelby County, TN. *Source:* Adapted from González et al. (2016).

deterministic estimate of the travel time from c to  $c^\prime$  using a separate transportation network.

In the transportation network, each edge has an associated length and speed limit, and its traversal time  $d_l$  is estimated assuming it will always be possible to travel at the speed limit. The deterministic estimate of  $tt_{cc'}^{\psi}$ , hereafter denoted as  $dtt_{cc'}^{\psi}$ , is obtained by determining the shortest path length between two nodes in the transportation network, namely those that are the closest to the midpoint of failed arcs and to failed nodes in the utility networks. To represent the uncertainty of  $tt_{cc'}^{\psi}$ , we populate a distribution for traversal time of edges in the transportation network; given  $d_l$ , the random traversal time  $dr_l$  is distributed according to the probability mass function:

$$P(dr_l = t) = \begin{cases} 0.3, & t = d_l \\ 0.3, & t = 1.5 \ d_l \\ 0.4, & t = 2 \ d_l \end{cases}$$
 (71)

and each scenario-indexed  $tt^{\psi}_{cc'\omega}$  is found by solving the shortest path problem as explained. This approach follows other disaster relief and emergency response studies with the assumption that random traversal times are based on a coefficient multiplication of the transportation network constant traversal times (Mete and Zabinsky, 2010; de la Torre et al., 2012; Alkhaleel et al., 2022).

#### 4.3. Parameters and computational information

Among the hypothetical earthquake scenarios in Shelby County, TN presented by González et al. (2016) with different magnitudes, assuming different failure probabilities of system components with each hypothetical earthquake scenario, we consider two possible scenarios with magnitudes  $M_w \in \{6,7\}$  and a similar number of disrupted components chosen randomly. Additionally, we consider four different risk coefficients (i.e.,  $\zeta \in \{0,0.5,1,2\}$ ) associated with each scenario. The number of disrupted components for each network, the percentage of the total number of components for each network, and the associated performance drop for each network in the system under each hypothetical earthquake scenario are summarized in Table 1.

Regarding repair activities, the shape and scale parameters of the Weibull distributed repair time are assumed to be 2 and 5, respectively, for all the components. Such assumptions are made following other studies in the literature in terms of probability distribution chosen and parameters (Fang and Sansavini, 2019). Hence, the mean-timeto-repair (MTTR) used in the deterministic model is about 4.43 h. In addition, the restoration planning horizon T is chosen as 20 h, which is sufficient to restore the network performance to its original state under both cases with the chosen number of work crews for each case (total of 4 for case 1 and 5 for case 2 as illustrated in Table 3). For possible repair modes for each network, it is assumed that there are two repair modes for each network  $(Y^{\psi} = \{1,2\})$ : (1) perfect repair mode (i.e., the component is restored to its full capacity), and (2) imperfect repair mode (i.e., the component is restored to 50% of its full capacity). Regarding cost parameters, it is assumed that unitary flow cost, unitary unsatisfied demand cost, and fixed repair cost per component are the same for both networks. For unitary flow cost, we use an estimated flow cost of \$30 per flow unit, which is equivalent to the approximate cost of transmission and distribution of 1 MWh of electricity (Fares and King, 2017). For the unsatisfied demand cost, referred to as disruption cost hereafter, the average residential cost of one MWh of electricity in Shelby County, TN is approximately \$97.2; and for the water network, the cost per 10k gallon is about \$30 (Memphis Light, Gas and Water Division (MLGW), 2021). However, the economic impact of unsatisfied demand is significantly higher than the cost of services. That is, estimates of service interruption vary significantly with estimated numbers ranging from \$100 up to \$100,000 per demand unit (Wolfram, 2021). Here, it is estimated to be about \$10,000 per demand unit based on the Interruption Cost Estimate (ICE) tool funded by the Energy Resilience Division of the U.S. Department of Energy's Office of Electricity (OE) for the examined case study area (Laboratory and Nexant, 2021). Regarding restoration costs, we assume a fixed repair cost per component. However, repair cost per CI component can vary significantly from thousand dollars to hundreds of million dollars (HDR, 2012; Assad et al., 2020). Nonetheless, a fixed repair cost of \$500,000 per component was estimated to keep both the flow and restoration costs combined lower than the disruption costs to prioritize resilience improvement as the main objective. Table 2 summarizes the parameters of cost, risk, and repair for each case.

For the scenario generation process of random variables (i.e., repair and travel times), 1000 scenarios are generated for each case. After that, the scenario reduction algorithm was used to reduce the number of scenarios into a smaller set. The total number of scenarios is reduced to 10 scenarios. Solutions to the MILPs used in the scenario reduction procedure and the stochastic optimization models were computed using CPLEX 12.10 (CPLEX, 2021) and programmed using Python

**Table 1**Disruption size and performance drop considering the two magnitudes of hypothetical earthquake scenarios.

Case	No. of disrupted components		Disruption	Disruption percentage			Performance drop		
	Power	Water	System	Power	Water	System	Power	Water	System
Case 1 ( $M_w = 6$ )	10	6	16	7.35%	5.00%	6.25%	18.64%	20.00%	19.27%
Case 2 $(M_w = 7)$	19	10	29	13.97%	8.33%	11.33%	22.13%	85.64%	50.87%

Table 2
Parameters of cost, risk, and repair for each case of the hypothetical earthquake scenarios.

Case Cost parameters		Risk parameters		Repair parameters			
	Disruption cost (per demand unit)	Repair cost (per component)	Flow cost (per flow unit)	α	ζ	$\chi_y^{\psi}$	$\nu_c$ , $\beta_c$
Case 1 $(M_w = 6)$ Case 2 $(M_w = 7)$	\$10,000	\$500,000	\$30	0.9 0.8	0, 0.5, 1, 2	$\chi_1^{\psi} = 0.5, \ \chi_2^{\psi} = 1$	5, 2

Table 3
Problem size of different study instances

Instance	No. of continuous variables	No. of binary variables	No. of constraints	No. of Scenarios	No. of work crews (power, water)	Number of repair modes (power, water)	Max computational time (s)
Case 1 $(M_w = 6)$	336,971	359,372	503,670	10	2,2	2,2	21,000
Case 2 $(M_w = 7)$	406,511	428,572	608,850	10	2,3	2,2	21,000
Deterministic (Case 1)	33,696	36,182	51,002	1	2,2	2,2	1,800
Deterministic (Case 2)	40,647	43,686	61,043	1	2,3	2,2	3,600

3.7 (Python, 2021) on a 3.2 GHz Intel Core i5 iMac machine with 24 GB of RAM.

Regarding solution times and optimality gaps, we would like to emphasize that solving ICIs deterministic restoration problems using commercial MILP solvers such as CPLEX is hard, especially for large problem instances involving travel time and vehicle routing considerations (Garay-Sianca and Pinkley, 2021; Moreno et al., 2019; Morshedlou et al., 2018). In such deterministic problems, optimality gaps can go up to 50% or even higher (Morshedlou et al., 2018; Garay-Sianca and Pinkley, 2021). Hence, the stochastic problem instances considered here for both cases cannot be solved for optimality within a prescribed time limit. However, based on our preliminary analysis, a time limit of 6 h (21600 s) is the approximate time after which the optimality gap tends to level off with the implementation of Benders algorithm to solve all instances. Algorithm 1 was implemented using callbacks with Benders cuts added as lazy constraints. Table 3 summarizes the dimensions of problem instances.

## 4.4. Results

The first part of this section summarizes the results related to the various features of the developed mean-risk model including a comparison of the proposed solution approach to standard MILP solvers, and the second part shows the added benefit of implementing flexible restoration strategies and PFI in total cost reduction and resilience improvement.

#### 4.4.1. Mean-risk model

The developed ICINRP using a mean-risk measure is solved using Algorithm 1. Table 4 compares the proposed Benders decomposition algorithm with CPLEX showing the added value of the proposed solution algorithm. The solutions found by the decomposition algorithm outperformed the ones found by CPLEX in all instances. Additionally, the decomposition algorithm was capable of solving all instances with a maximum optimality gap of about 24%. In contrast, CPLEX was not able to find any feasible solution for one of the instances (i.e.,  $M_w = 6$  ( $\zeta = 0.5$ )). The maximum optimality gap of solved instances for CPLEX was approximately 57%. It is worth pointing out that the lower bounds found by CPLEX and the decomposition algorithm for the instances were similar, which are higher (tighter) than the WSs lower bounds by about 10% for all instances. For the first case ( $M_w = 6$ ), the

highest optimality gap found using Benders decomposition algorithm was 14.637% compared to more than triple that value at 50%.456 for CPLEX. Furthermore, in the second case ( $M_w=7$ ), the highest optimality gap found using Benders decomposition algorithm was 23.319% compared to 56.88% for the commercial solver. Using the proposed Benders algorithm, the average optimality gaps for cases 1 and 2 were about 13% and 20%, respectively. In contrast, the average optimality gaps using CPLEX solver for cases 1 and 2 were about 32% and 46%, respectively. These average values are about double the average gaps of the decomposition algorithm. Overall, these findings favor the proposed solution approach and show the added benefit of adapting it over commercial solvers.

Regarding the mean-risk model, the choice of the risk coefficient  $\zeta$  in the proposed framework can alter the optimal plan; that is, increasing the value of  $\zeta$  increases the relative importance of the risk term resulting in more conservative (risk-averse) plans. For instance, the CVaR values for case 1 showed a significant decrease with the increase of the risk coefficient value from 0 to 2 as shown in Fig. 3. This decrease in CVaR values is associated with a gradual increase in the expected total cost across scenarios for the different risk coefficients as illustrated in Fig. 3. The same findings are true for case 2 with a steeper trend in CVaR values as shown in Fig. 4.

In ICINs restoration problems, disruption costs are expected to be higher than other costs combined, otherwise the optimal solutions can be found by prioritizing a reduction in the repair and flow costs over the disruption costs (Almoghathawi et al., 2021). Here, the detailed costs are presented for both cases in Figs. 3 and 4 showing that disruption cost constitutes the major portion of the total cost under all risk coefficients. Note that the total cost term here represents only the total of disruption cost, repair cost and flow cost and is different than the objective value term, which includes the total cost and CVaR terms inflated by the risk importance factor. In addition, trends of objective values, total and disruption costs, and CVaR values under both cases across the different risk coefficients are shown in Figs. 5 and 6; this shows that in mean-risk models, the objective value increases linearly with the increase of the risk coefficient. Moreover, both the expected total cost and disrupted cost exhibit similar raising trends as the risk coefficient changes. This similarity can be explained by knowing that the disruption cost represents the major portion of the total cost as explained earlier.

Table 4

Comparison of Benders decomposition and CPLEX solver solutions for the different instances with 10 reduced scenarios.

Case	CPLEX standard solver			Benders decomposition			
	Computational time (s)	Gap(%)	Objective value	Computational time (s)	Gap(%)	Objective value	
$M_w = 6 \ (\zeta = 0)$	21648.783	17.279	18.142	21617.794	12.849	17.514	
$M_w = 6 \ (\zeta = 0.5)$	21600.000	_	_	21618.569	14.477	30.599	
$M_w = 6 \ (\zeta = 1)$	21605.193	50.456	58.771	21616.394	14.637	42.986	
$M_w = 6 \ (\zeta = 2)$	21609.664	29.233	81.635	21661.764	12.791	66.632	
$M_w = 7 \ (\zeta = 0)$	21612.699	56.880	90.808	21664.057	23.319	47.302	
$M_w = 7 \ (\zeta = 0.5)$	21606.937	38.043	96.661	21615.361	21.666	75.205	
$M_w = 7 \ (\zeta = 1)$	21612.841	41.277	143.474	21614.859	20.328	102.743	
$M_w = 7 \ (\zeta = 2)$	21607.326	50.304	271.706	21620.736	17.480	154.189	

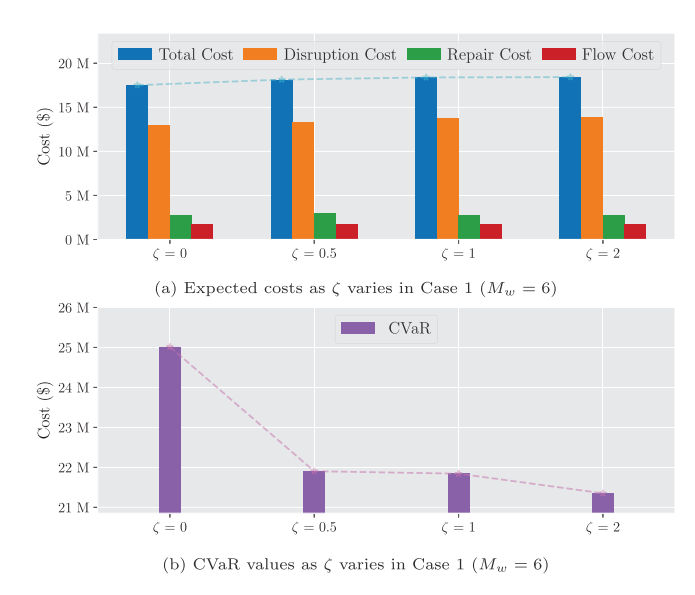


Fig. 3. Case 1 ( $M_w=6$ ): Detailed expected cost values of demand, repair, flow, and the overall expected total cost, as well as the CVaR information for different values of  $\zeta$ .

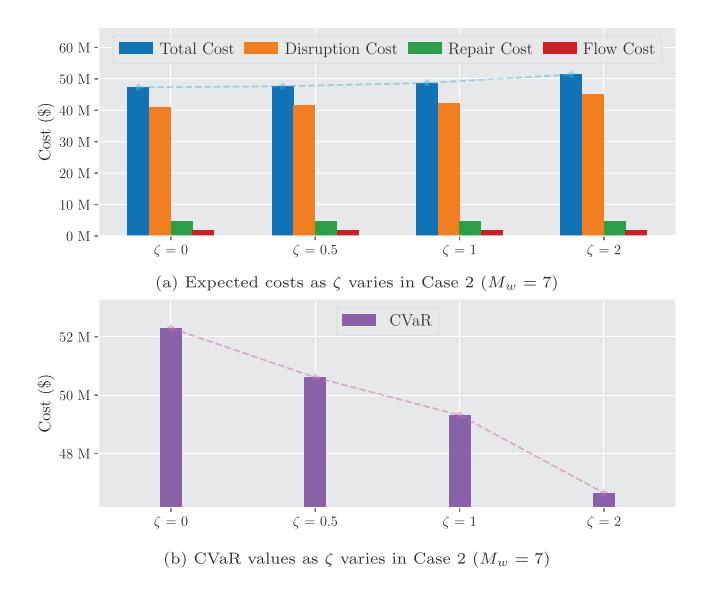


Fig. 4. Case 2 ( $M_w=7$ ): Detailed cost values of demand, repair, flow, and the overall expected total cost, as well as the CVaR information for different values of  $\zeta$ .

Tables 5 and 6 summarize the detailed outputs of the model for both cases – considering different choices of risk coefficient – including cost values, system and individual network resilience values, objective values, and other outputs for both cases. For case 1, the total resilience (or system resilience) decreases whereas the total disruption cost increases as the risk coefficient increases. The repair cost, however, looks constant across all risk coefficients indicating that the number of chosen disrupted components to be restored and their associated repair modes are almost the same for case 1. For case 2, the repair cost shows a similar behavior across all the values of  $\zeta$ . Additionally, the flow cost could be described as a constant across the values of  $\zeta$  for both cases. The resilience curves of the power network, water network, and system under the different risk coefficients can be found in Appendix.

To assess the added value of stochastic models compared to a deterministic approach, the value of stochastic solution (VSS) is a wellknown measure in the literature, which is designed to indicate whether the added benefit of modeling randomness using a risk-neutral stochastic optimization approach (Birge and Louveaux, 2011). However, the VSS cannot be implemented directly on risk-averse problems (Noyan, 2012). Accordingly, we adopt the risk-averse version of the VSS known as the mean-risk value of stochastic solution (MRVSS) (see Noyan, 2012 for details), which measures the possible gain from solving stochastic models incorporating a mean-risk function. In particular, this measure represents the difference between the mean-risk expected value (MREV) problem (which results from solving the standard model with fixed first-stage decision variables whose values are obtained by solving a deterministic version of the standard model that replaces all random parameters with their expected values) and the mean-risk standard model solution. Higher values of MRVSS indicate a more added value in adapting a mean-risk approach over an expected value approach. Note that the MRVSS is equivalent to VSS when the risk coefficient  $\zeta = 0$ .

For case 1 ( $M_w = 6$ ), it can be seen that the MRVSS values are positive numbers ranging between 2.285M and 10.295M and increase with the increase of the risk coefficient  $\zeta$ ; this indicates the significance of solving mean-risk models over the expected value (deterministic) approaches. However, the increase of MRVSS with  $\zeta$  is not reflected on the ratio between the MRVSS and the associated objective value, which does not show a clear trend with approximate values of 13%, 11%, 12%, and 15% for  $\zeta = 0$ , 0.5, 1, and 2, respectively. For  $\zeta = 0$ , the added value of a stochastic solution is \$2.285M (i.e., the overall cost of the deterministic solution is \$2.285M higher than the stochastic solution). For other values of  $\zeta$ , the MRVSS varies between a  $\zeta$ -weighted value of 3M up to 10M. For case 2 ( $M_w = 7$ ), the values of MRVSS are even higher given the larger disruption scenario for this case despite the higher overall optimality gaps in this case compared to case 1. In fact, implementing the deterministic approach for this case can cause a 10%-20% increase in the expected economic losses compared to a mean-risk plan with a specific risk level  $\alpha$  and risk weighted importance  $\zeta$ . Hence, this shows that applying deterministic plans for larger disruptions involves high risk and could result in more economic losses. Overall, these results indicate that it is significant to solve meanrisk models to obtain preferred solutions for a specified set of risk parameters.

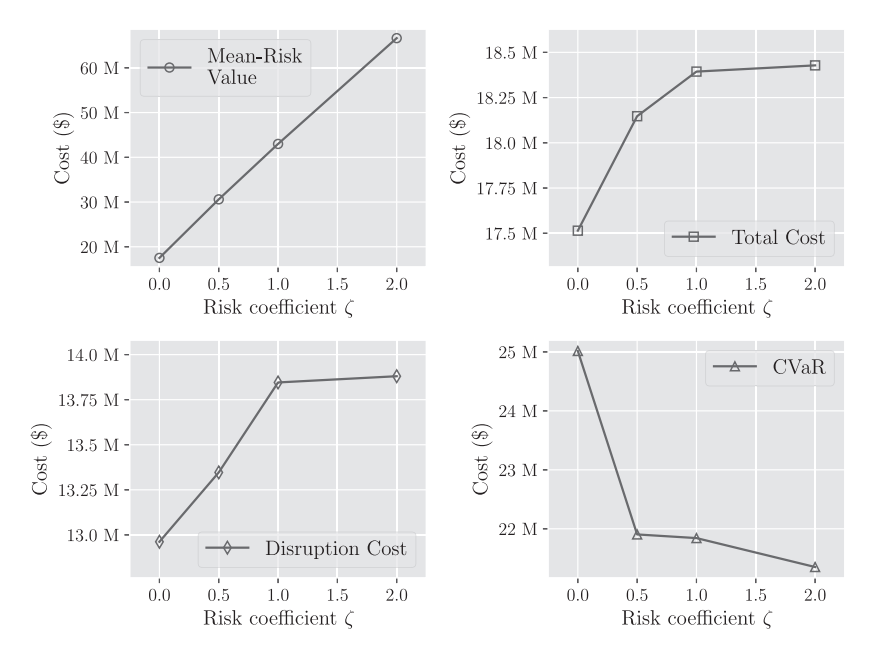


Fig. 5. Case 1 ( $M_w = 6$ ): Trends of objective value, expected total cost, expected disruption cost, and CVaR with the increase of  $\zeta$ .

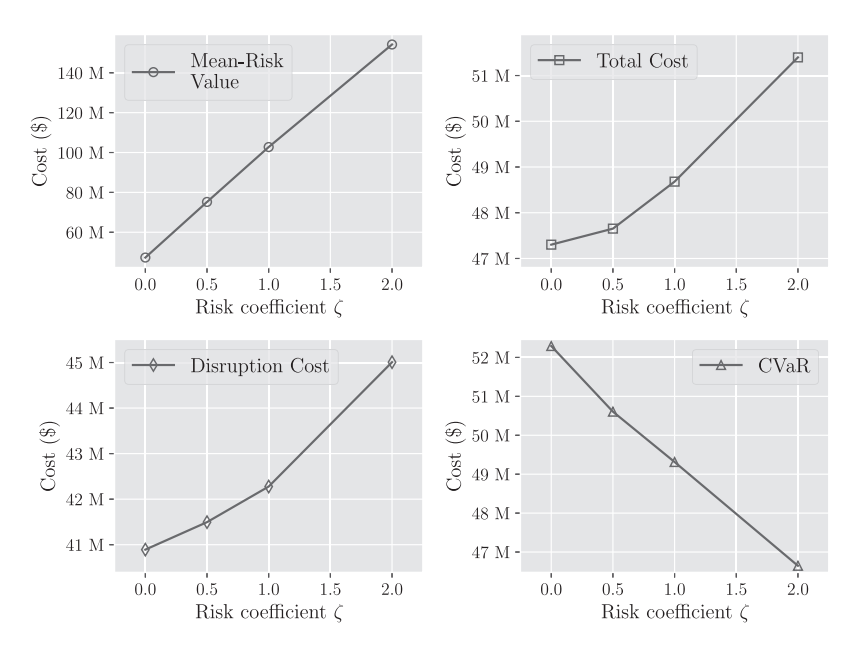


Fig. 6. Case 2 ( $M_w$  = 7): Trends of objective value, expected total cost, expected disruption cost, and CVaR with the increase of  $\zeta$ .

### 4.4.2. Flexible restoration strategies and PFI

As illustrated in Section 2, the proposed optimization model for solving the ICINRP considers flexible restoration strategies that are expected to enhance the resulting optimal plans. In addition, the proposed model allows for partial functioning and interdependency, with a slight modification to the standard model formulation, supporting non-binary state ICIs restoration. Here, we compare the applied flexible restoration strategies to restricted ones and study the impact of PFI on restoration plans.

Regarding the restoration strategies, Tables 7 and 8 summarize the detailed outputs (i.e., cost values, system and individual network resilience values, and CVaR values) of the model with risk coefficient  $\zeta = 1$  under flexible (i.e., multicrew and multimode repair settings) and restricted (i.e., single crew and single mode settings) plans for cases 1 and 2, respectively. In Tables 7 and 8, the first column represents the

standard model with  $\zeta=1$ , the second column represents the standard model with  $\zeta=1$  except that each failed component is restored by at most one crew (single crew setting), the third column represents the standard model with  $\zeta=1$  except that each failed component can only be fully restored (single repair mode), and the PFI column represents the standard model with  $\zeta=1$  except that partial functioning and interdependencies are allowed. Overall, both the objective value and CVaR value are lower under flexible restoration strategies for cases 1 and 2. This indicates that flexible restoration planning can significantly reduce the main costs associated with restoration, namely disruption and repair costs, as well as the associated risk measure. Comparing the multicrew setting to the single crew setting, the reduction in the objective value is about 25% and 36% for cases 1 and 2, respectively. For multimode repair vs. single mode repair, the reduction in the objective value is approximately 12% and 20% for cases 1 and 2, respectively.

Table 5 Case 1 ( $M_w = 6$ ): Detailed expected costs, MRVSS, expected flow, and expected resilience information considering different risk coefficients.

	Risk coefficient parameter					
	$\zeta = 0$	$\zeta = 0.5$	$\zeta = 1$	$\zeta = 2$		
Objective value (M)	17.514	30.599	42.986	66.632		
CVaR (\$M)	25.016	21.904	21.843	21.352		
MRVSS (M)	2.285	3.417	4.962	10.295		
Total disruption cost (\$M)	12.962	13.347	13.846	13.880		
Total repair cost (\$M)	2.750	3.000	2.750	2.750		
Total flow cost (\$M)	1.803	1.801	1.798	1.798		
Total cost (\$M)	17.515	18.148	18.394	18.428		
Total resilience	0.816	0.810	0.805	0.804		
Power network disruption cost (\$M)	6.707	6.729	7.945	7.879		
Power network repair cost (\$M)	1.750	2.250	2.000	2.000		
Power network flow cost (\$M)	0.989	0.989	0.983	0.983		
Power network resilience	0.821	0.820	0.788	0.789		
Power network aggregated received flow (MWh)	19389.300	19387.118	19265.504	19272.070		
Water network disruption cost (\$M)	6.255	6.618	5.901	6.001		
Water network repair cost (\$M)	1.000	0.750	0.750	0.750		
Water network flow cost (\$M)	0.814	0.812	0.815	0.815		
Water network resilience	0.812	0.801	0.822	0.819		
Water network aggregated received flow (MG)	159.545	159.182	159.899	159.799		

Table 6 Case 2 ( $M_w = 7$ ): Detailed expected cost values, MRVSS, expected flow, and expected resilience information under different risk coefficients.

	Risk coefficient parameter				
	$\zeta = 0$	$\zeta = 0.5$	$\zeta = 1$	$\zeta = 2$	
Objective value(M)	47.302	75.205	102.743	154.189	
CVaR (\$M)	52.293	50.606	49.313	46.646	
MRVSS (M)	9.678	10.415	16.287	16.772	
Total disruption cost (\$M)	40.892	41.495	42.277	45.007	
Total repair cost (\$M)	4.750	4.500	4.750	4.750	
Total flow cost (\$M)	1.660	1.657	1.653	1.639	
Total cost (\$M)	47.302	47.652	48.680	51.396	
Total resilience	0.757	0.726	0.752	0.725	
Power network disruption cost (\$M)	16.402	16.474	12.786	14.996	
Power network repair cost (\$M)	2.500	2.500	2.500	2.500	
Power network flow cost (\$M)	0.939	0.939	0.958	0.947	
Power network resilience	0.686	0.629	0.712	0.662	
Power network aggregated received flow (MWh)	18419.820	18412.648	18781.405	18560.355	
Water network disruption cost (\$M)	24.490	25.022	29.491	30.011	
Water network repair cost (\$M)	2.250	2.000	2.250	2.250	
Water network flow cost (\$M)	0.721	0.718	0.695	0.693	
Water network resilience	0.828	0.824	0.792	0.789	
Water network aggregated received flow (MG)	141.310	140.778	136.309	135.789	

Table 7 Case 1 ( $M_w = 6$ ): Detailed cost values, flow, and resilience information under SC, SM, and PFI for  $\zeta = 1$ .

	Standard Model ( $\zeta = 1$ )	Single Crew	Single Repair Mode	PFI
Objective value (M)	42.986	57.604	48.968	29.463
CVaR (\$M)	21.843	29.642	25.773	14.381
Total disruption cost (\$M)	13.846	20.699	15.405	7.753
Total repair cost (\$M)	2.750	2.750	3.000	2.750
Total flow cost (\$M)	1.798	1.763	1.790	1.829
Total resilience	0.805	0.712	0.781	0.893
Power network disruption cost (\$M)	7.945	14.127	7.946	5.506
Power network repair cost (\$M)	2.000	2.000	2.000	2.250
Power network flow cost (\$M)	0.983	0.951	0.983	0.995
Power network resilience	0.788	0.622	0.788	0.853
Power network aggregated received flow (MWh)	19265.504	18647.284	19265.372	19509.405
Water network disruption cost (\$M)	5.901	6.571	7.459	2.247
Water network repair cost (\$M)	0.750	0.750	1.000	0.500
Water network flow cost (\$M)	0.815	0.812	0.808	0.834
Water network resilience	0.822	0.802	0.775	0.932
Water network aggregated received flow (MG)	159.899	159.229	158.341	163.553

Table 8 Case 2 ( $M_w = 7$ ): Detailed cost values, flow, and resilience information under SC, SM, and PFI for  $\zeta = 1$ .

	Standard Model ( $\zeta = 1$ )	Single Crew	Single Repair Mode	PFI
Objective value (M)	102.743	161.303	128.854	83.569
CVaR (\$M)	49.313	83.061	61.543	39.845
Total disruption cost (\$M)	42.277	67.719	52.712	32.521
Total repair cost (\$M)	4.750	4.500	6.500	4.750
Total flow cost (\$M)	1.653	1.523	1.600	1.703
Total resilience	0.752	0.613	0.684	0.788
Power network disruption cost (\$M)	12.786	19.160	16.831	12.551
Power network repair cost (\$M)	2.500	2.250	3.500	2.500
Power network flow cost (\$M)	0.958	0.925	0.937	0.959
Power network resilience	0.712	0.568	0.621	0.717
Power network aggregated received flow (MWh)	18781.405	18144.010	18376.940	18804.894
Water network disruption cost (\$M)	29.491	48.559	35.881	19.970
Water network repair cost (\$M)	2.250	2.250	3.000	2.250
Water network flow cost (\$M)	0.695	0.598	0.663	0.744
Water network resilience	0.792	0.658	0.747	0.859
Water network aggregated received flow (MG)	136.309	117.241	129.919	145.830

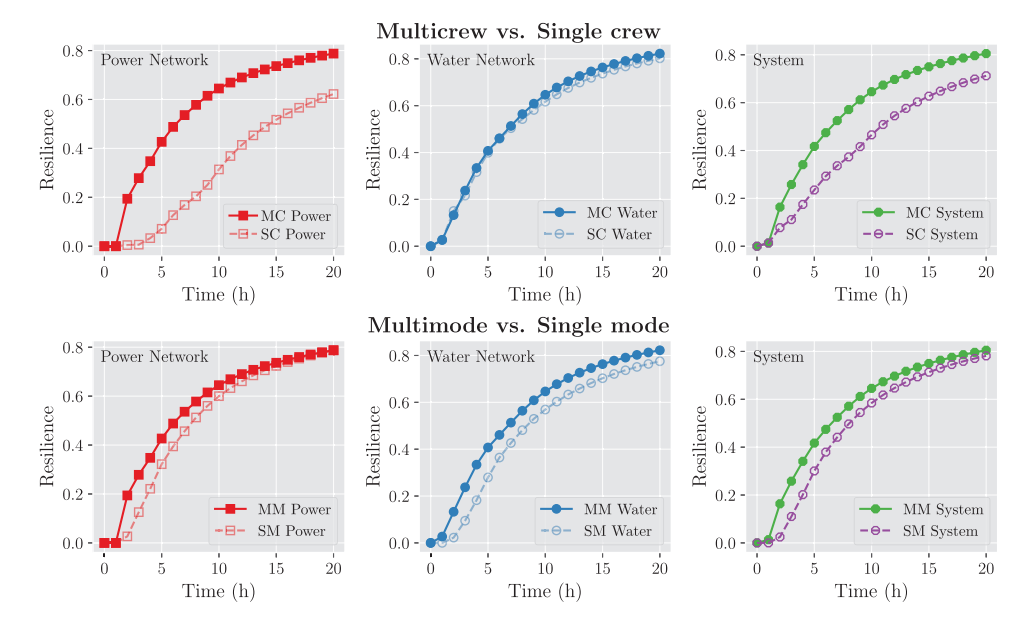


Fig. 7. Case 1 ( $M_w = 6$ ): Comparison of the resilience of the overall system and individual networks under SC vs. MC, and SM vs. MM settings.

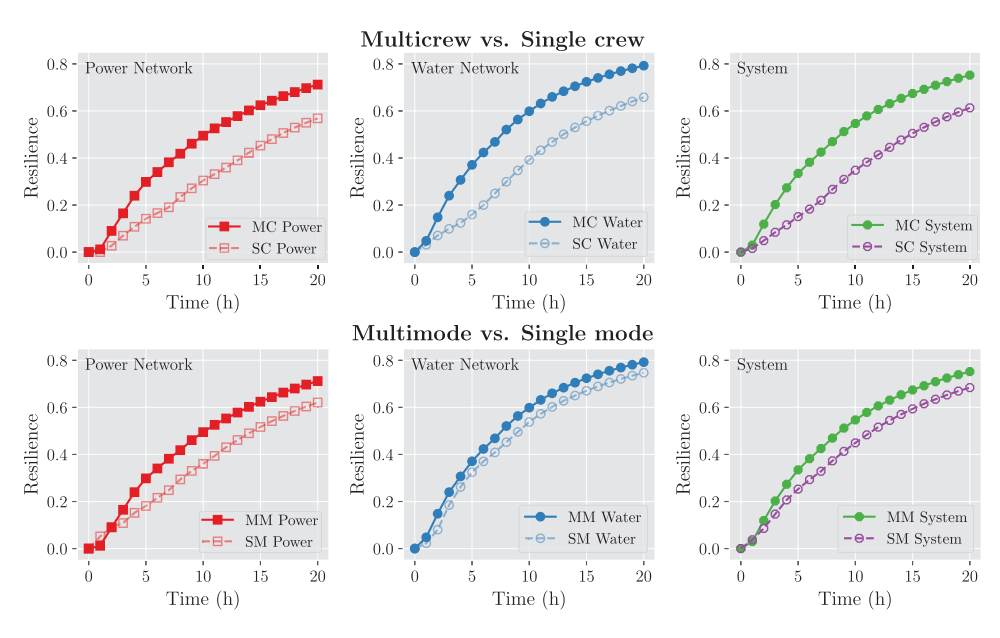


Fig. 8. Case 2 ( $M_w = 7$ ): Comparison of the resilience of the overall system and individual networks under SC vs. MC, and SM vs. MM settings.

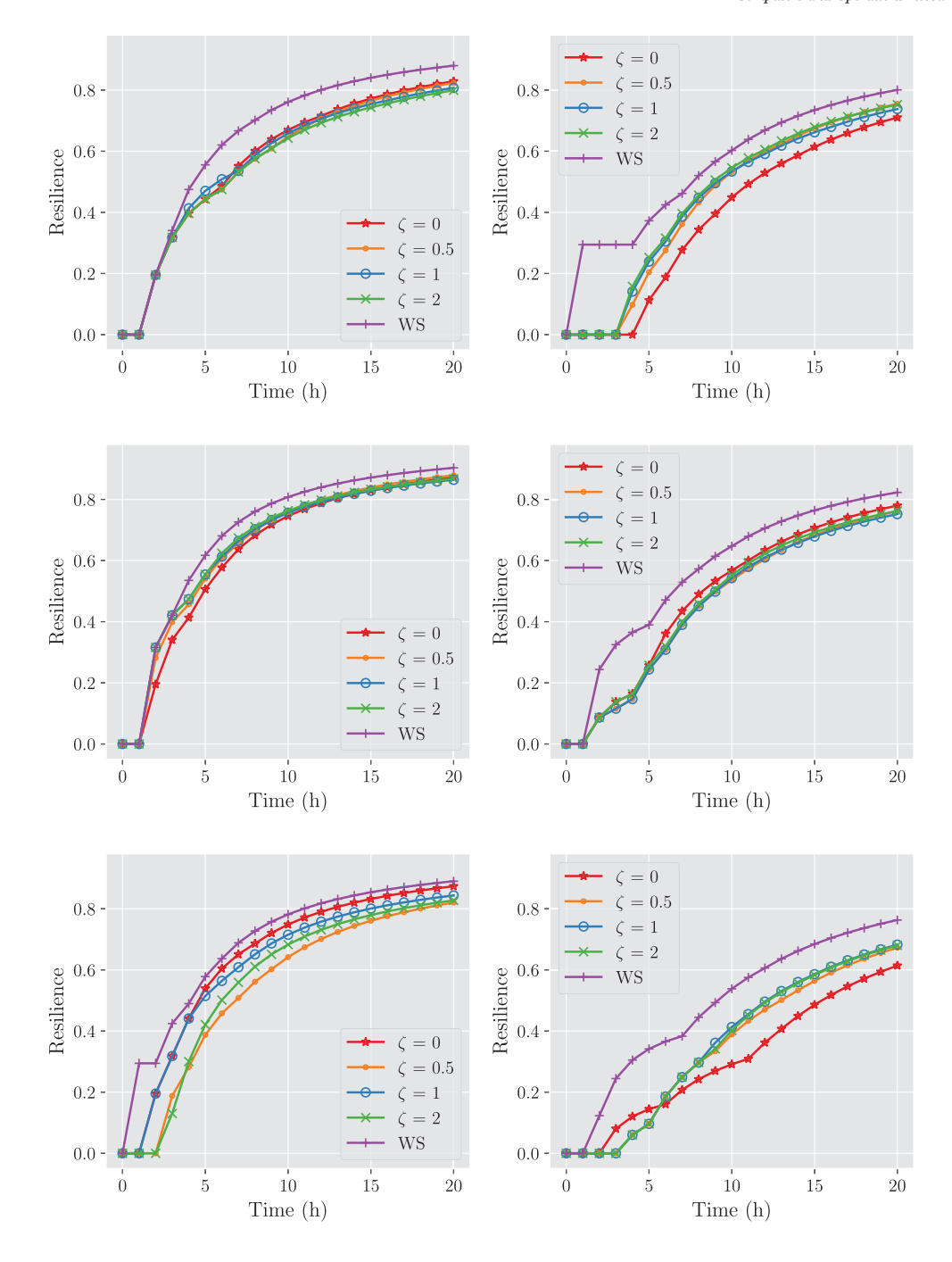


Fig. A.1. Case 1 (M<sub>w</sub> = 6): Comparison of system resilience curves under different risk coefficient solution plans for a sample of reduced scenarios.

Note that the gain from adapting flexible restoration strategies is more significant for the second case with a higher number of disrupted components. Disruption costs behave similarly to the objective value for both cases and under both restoration strategies (i.e., multicrew and multimode repair). In contrast, repair costs are similar between the multicrew and single crew settings; however, they are higher in the single repair mode setting, significantly higher for case 2, indicating that the imperfect repair mode for multiple components is optimal. Surprisingly, multimode repair did not only reduce the repair costs by %8 and 27% for cases 1 and 2, respectively, but also reduced the disruption costs (improved resilience) for both cases by 10% for case 1 and 20% for case 2.

For a resilience-based benchmarking of the different restoration strategies, a comparison of the resilience of power network, water network, and system under flexible and restricted restoration plans for cases 1 and 2 is shown in Figs. 7 and 8, respectively. From the first glance, one can see that the resilience of both networks and the system is higher with multicrew and multimode restoration strategies. For instance, in case 1, the power network resilience under multicrew setting is significantly higher than under a single crew setting. This indicates the existence of critical components in the power network whose rapid restoration can significantly improve the resilience of the network. In contrast, the effect of multicrew setting on the water network resilience is minor. Conversely, multimode repair improved only the resilience of the water network under the same case. For case 2, with a higher

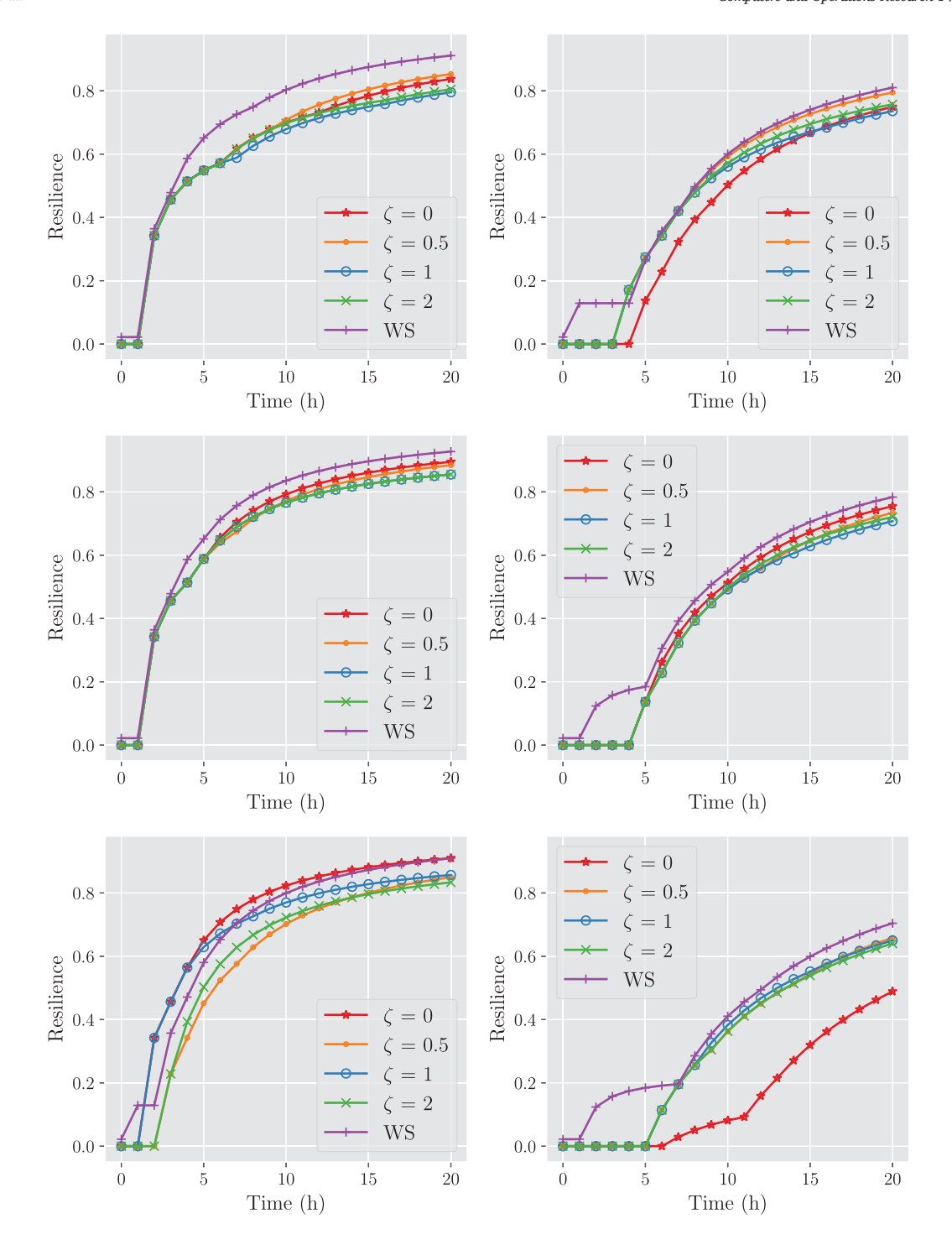


Fig. A.2. Case 1 ( $M_w = 6$ ): Comparison of power network resilience curves under different risk coefficient solution plans for a sample of reduced scenarios.

number of disrupted components, the resilience of both power and water networks showed a substantial improvement under multicrew and multimode settings. All these improvements in the resilience of both individual networks are clearly reflected on the system resilience for both case studies and under both flexible restoration strategies.

Regarding PFI, Tables 7 and 8 summarize the detailed outputs (i.e., cost values, system and individual network resilience values, and CVaR values) of the standard model, under risk coefficient  $\zeta=1$ , with and without PFI for both cases. It can be seen that partial functioning and interdependency significantly reduced the disruption costs for both

cases. That is, resilience is improved by PFI since allowing a disrupted component to partially function – before full restoration – can help deliver more flow to demand nodes, especially in the first time periods after disruption. This situation is the opposite of a binary status setting of components where disrupted components continue to be disrupted until fully restored. In addition, the reduction in disruption costs decreases the risk gradually compared to a non-PFI setting. The results from applying PFI can link resilience to reliability and maintainability engineering through systems with multiple states or state-dependent systems. It might be of interest to study the relation between resilience,

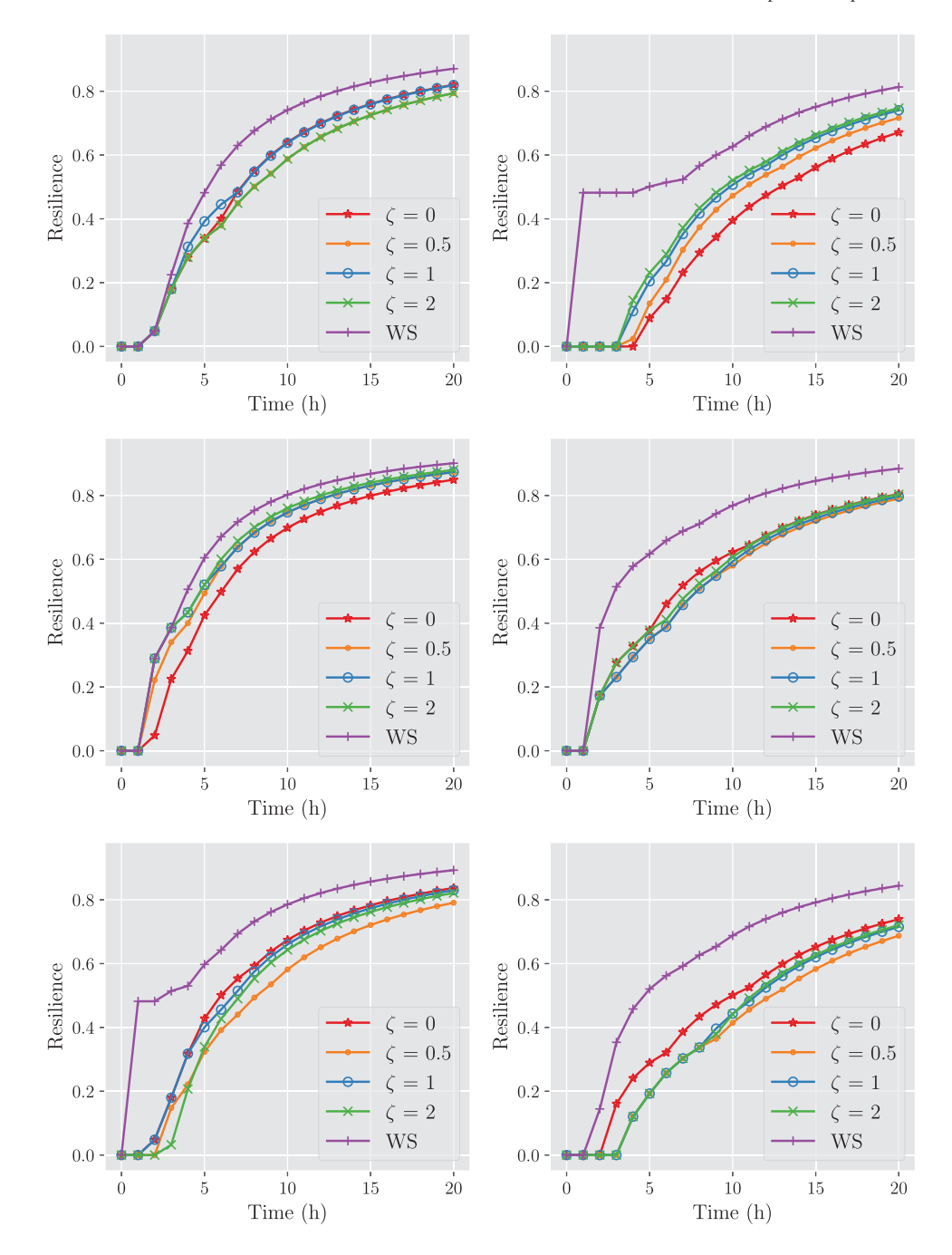


Fig. A.3. Case 1 (Mw = 6): Comparison of water network resilience curves under different risk coefficient solution plans for a sample of reduced scenarios.

reliability, and maintainability for a network having state-dependent critical components and how a tri-level framework can be developed to improve all three aspects. To sum up, ICINs systems featuring PFI are expected to be more resilient than non-PFI due to the flexibility of their post-disruption restoration plans.

### 5. Conclusion and future work

In this paper, a two-stage stochastic restoration optimization model using mixed-integer linear programming is proposed to solve the ICINRP under a mean-risk cost-based objective function. Moreover, the mean-risk model features flexible restoration planning strategies including multicrew repair of a single component and multimode repair, and

also considers partial functioning and interdependencies of components across networks. The proposed model: (i) determines the set of failed components to be restored, (ii) selects the repair mode for each failed component, (iii) assigns each crew the set of failed components to be restored individually or concurrently, (iv) and schedules the baseline restoration sequence across scenarios for each crew such that the associated costs of disruption, repair, and flow of the system of ICIs are minimized. Additionally, as post-disruption restoration tasks occur in a highly dynamic environment, which is subject to a fair amount of uncertainty, the mean-risk model considers two important sources of uncertainty associated with restoration panning: (i)repair task durations, and (ii)travel times of crews between failed components.

The proposed approach was demonstrated using a real-life case study based on the system of power and water networks in Shelby

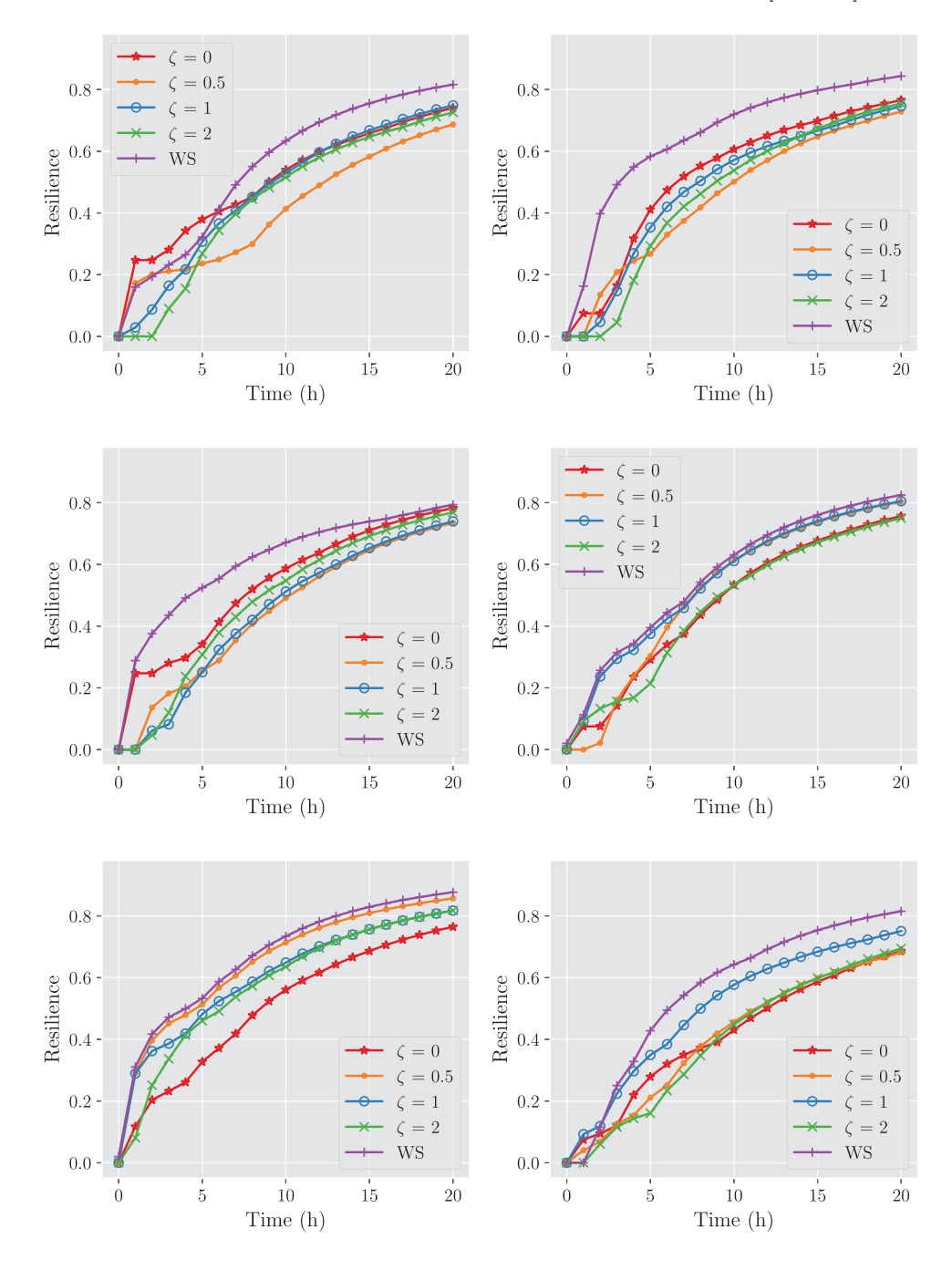


Fig. A.4. Case 2 (M<sub>w</sub> = 7): Comparison of system resilience curves under different risk coefficient solution plans for a sample of reduced scenarios.

County, TN, U.S. under two hypothetical earthquakes. The mean-risk model was solved using the developed Benders decomposition algorithm, which outperformed the CPLEX standard solver as demonstrated. Our first finding was the significance of adapting mean-risk stochastic models over deterministic counterparts. This was demonstrated through the positive values of MRVSS under all cases. It is also found that the restoration plan can be altered based on the associated risk weighted importance. In particular, smaller values of the risk weighted importance factor can result in plans with low expected total costs but with high costs under worst-case scenarios. In contrast, higher values of the risk weighted importance factor can result in plans with slightly higher expected total costs but with less costs associated with worst-case scenarios. Regarding the flexible restoration strategies and PFI,

both implementations demonstrated the added value in reducing the overall costs and mitigating risks.

As for future work, the proposed model could be extended to consider the transportation network as a direct interdependent network. That is, the current approach assumes that CI networks, other than the underlying transportation network, are the ones being restored. Hence, the problem becomes not only focused on the restoration of CIs, but also on coordinating the process of finding the best routes and schedules for crews to repair damaged components in the transportation network. In addition, it is possible to extend the current model to introduce a facility location problem where work crews are dispatched to disrupted component locations rather than a direct travel between components. In such problems, the goal is to find the optimal location of these facilities from a set of candidate sites considering the fixed cost of

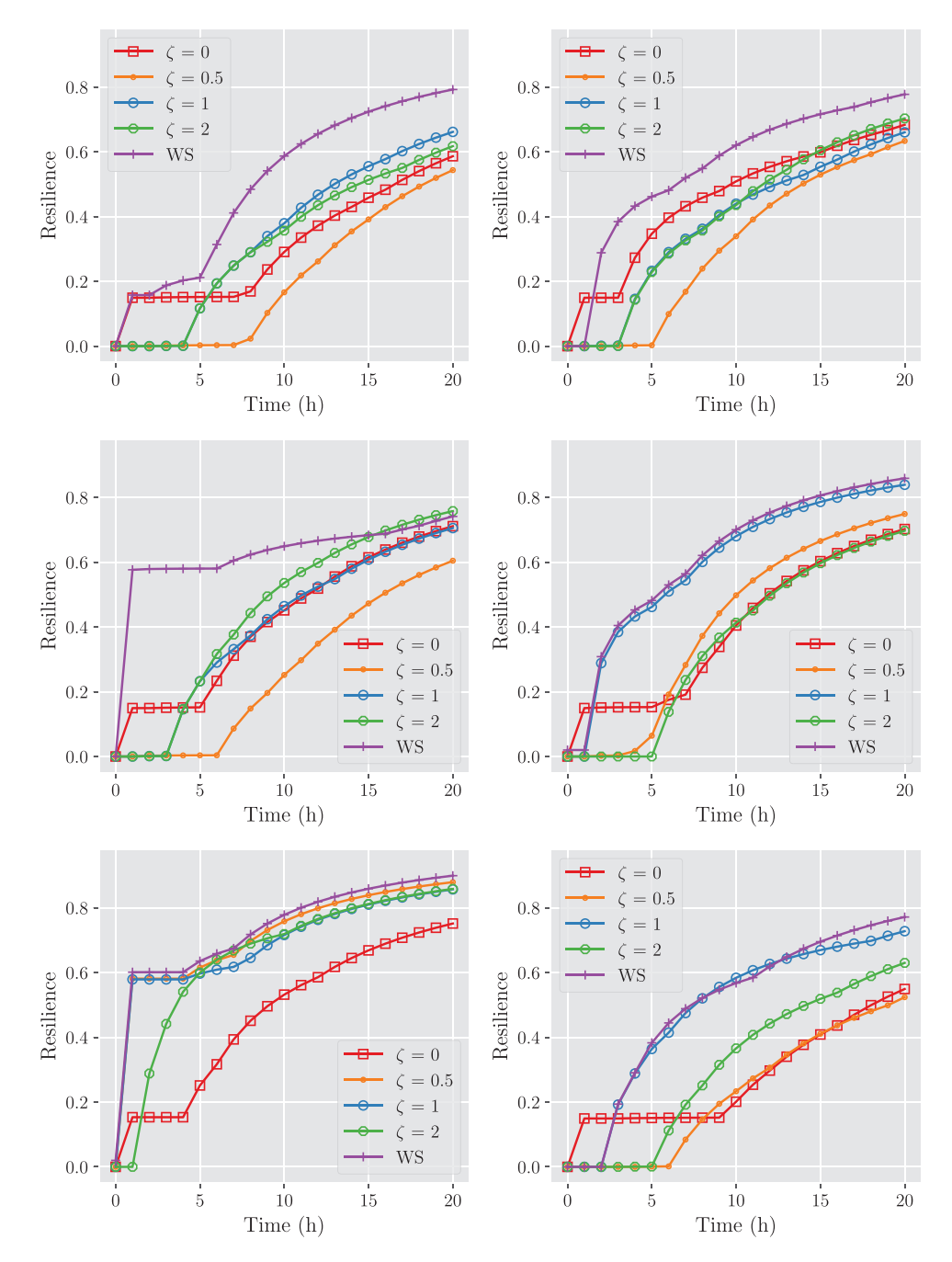


Fig. A.5. Case 2 (Mw = 7): Comparison of power network resilience curves under different risk coefficient solution plans for a sample of reduced scenarios.

establishing such facilities as well as other crew-related variable costs. Moreover, considering economic measures of the resilience of communities interacting with these ICINs, as well as the associated risks can be one of the future directions of this work. This future direction can also be associated with studying other types of interdependencies that affect both CIs and communities such as geographic interdependency to mitigate the related socioeconomic risks.

#### CRediT authorship contribution statement

Basem A. Alkhaleel: Conceptualization, Methodology, Formal Analysis, Writing. Haitao Liao: Conceptualization, Methodology, Writing – review & editing, Project administration. Kelly M. Sullivan: Conceptualization, Methodology, Writing – review & editing.

# Acknowledgments

The authors would like to thank the editors and anonymous reviewers for their constructive comments that have led to an improvement over an earlier version of this paper. This work was supported by the U.S. National Science Foundation under Grant No. OIA 2119691.

#### **Appendix**

A.1. Resilience of the system and individual infrastructure networks under different risk coefficient solution plans

See Figs. A.1-A.6.

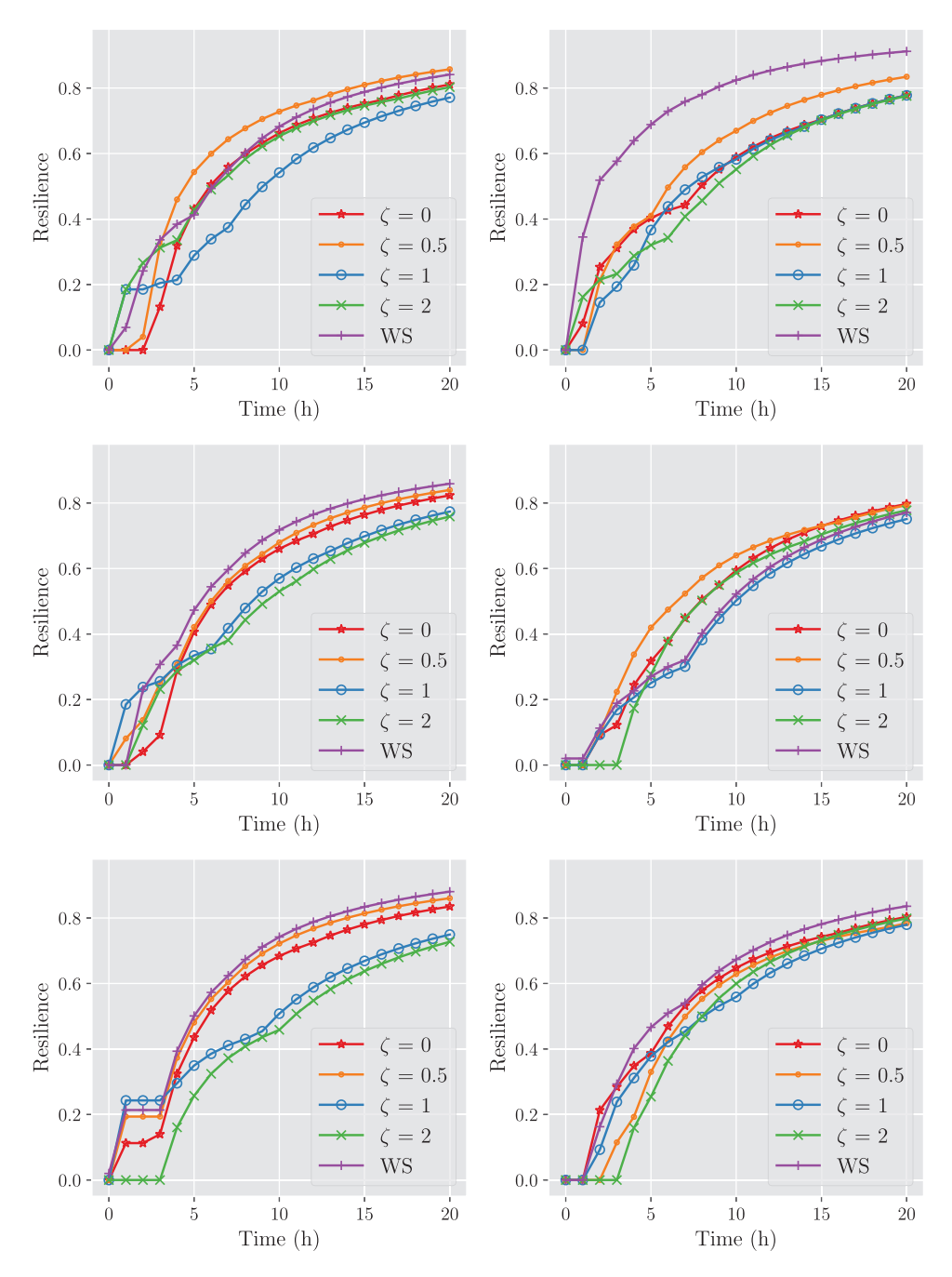


Fig. A.6. Case 2 (Mw = 7): Comparison of water network resilience curves under different risk coefficient solution plans for a sample of reduced scenarios.

#### References

Abdelkader, Y.H., 2004. Evaluating project completion times when activity times are Weibull distributed. European J. Oper. Res. 157 (3), 704–715.

Ahuja, R.K., Magnanti, T.L., Orlin, J.B., 1993. Network Flows: Theory, Algorithms, and Applications. Prentice-Hall, Inc., Upper Saddle River, NJ, USA.

Alkhaleel, B.A., Liao, H., Sullivan, K.M., 2022. Risk and resilience-based optimal post-disruption restoration for critical infrastructures under uncertainty. European J. Oper. Res. 296 (1), 174–202. http://dx.doi.org/10.1016/j.ejor.2021.04.025.

Almoghathawi, Y., Barker, K., Albert, L.A., 2019. Resilience-driven restoration model for interdependent infrastructure networks. Reliab. Eng. Syst. Saf. 185, 12–23.

Almoghathawi, Y., González, A.D., Barker, K., 2021. Exploring recovery strategies for optimal interdependent infrastructure network resilience. Netw. Spat. Econ. 21 (1), 229–260. http://dx.doi.org/10.1007/s11067-020-09515-4.

Amin, M., 2002. Toward secure and resilient interdependent infrastructures. J. Infrastructure Syst. 8 (3), 67–75. http://dx.doi.org/10.1061/(ASCE)1076-0342(2002)8: 3(67).

Assad, A., Moselhi, O., Zayed, T., 2020. Resilience-driven multiobjective restoration planning for water distribution networks. J. Perform. Constr. Facil. 34 (4), 04020072. http://dx.doi.org/10.1061/(asce)cf.1943-5509.0001478.

Azucena, J., Alkhaleel, B., Liao, H., Nachtmann, H., 2021. Hybrid simulation to support interdependence modeling of a multimodal transportation network. Simul. Model. Pract. Theory 107, 102237. http://dx.doi.org/10.1016/j.simpat.2020.102237.

Baidya, P.M., Sun, W., 2017. Effective restoration strategies of interdependent power system and communication network. J. Eng. 2017 (13), 1760–1764. http://dx.doi.org/10.1049/joe.2017.0634.

Barker, K., Lambert, J.H., Zobel, C.W., Tapia, A.H., Ramirez-Marquez, J.E., Albert, L., Nicholson, C.D., Caragea, C., 2017. Defining resilience analytics for interdependent cyber-physical-social networks. Sustain. Resilient Infrastructure 2 (2), 59–67. http://dx.doi.org/10.1080/23789689.2017.1294859.

Benders, J.F., 1962. Partitioning procedures for solving mixed-variables programming problems. Numer. Math. 4, 238–252.

Birge, J.R., Louveaux, F., 2011. Introduction to Stochastic Programming. Springer, New York, NY.

Bruneau, M., Chang, S.E., Eguchi, R.T., Lee, G.C., O'Rourke, T.D., Reinhorn, A.M., Shinozuka, M., Tierney, K., Wallace, W.A., von Winterfeldt, D., 2003. A framework

- to quantitatively assess and enhance the seismic resilience of communities. Earthq. Spectra 19, 733–752. http://dx.doi.org/10.1193/1.1623497.
- Bruninx, K., 2014. A practical approach on scenario generation and & reduction algorithms for wind power forecast error scenarios.
- Buldyrev, S.V., Parshani, R., Paul, G., Stanley, H.E., Havlin, S., 2010. Catastrophic cascade of failures in interdependent networks. Nature 464 (7291), 1025–1028. http://dx.doi.org/10.1038/nature08932.
- Buldyrev, S.V., Shere, N.W., Cwilich, G.A., 2011. Interdependent networks with identical degrees of mutually dependent nodes. Phys. Rev. E 83 (1), 016112. http://dx.doi.org/10.1103/physreve.83.016112.
- Campbell, R.J., Lowry, S., 2012. Weather-Related Power Outages and Electric System Resiliency. Library of Congress, Washington, DC.
- Casalicchio, E., Galli, E., Ottaviani, V., 2009. MobileOnRealEnvironment-GIS: A federated mobile network simulator of mobile nodes on real geographic data. In: 2009 13th IEEE/ACM International Symposium on Distributed Simulation and Real Time Applications. IEEE, http://dx.doi.org/10.1109/ds-rt.2009.25.
- Cavdaroglu, B., Hammel, E., Mitchell, J.E., Sharkey, T.C., Wallace, W.A., 2011. Integrating restoration and scheduling decisions for disrupted interdependent infrastructure systems. Ann. Oper. Res. 203 (1), 279–294. http://dx.doi.org/10.1007/s10479-011-0959-3.
- Çelik, M., 2016. Network restoration and recovery in humanitarian operations: Framework, literature review, and research directions. Surv. Oper. Res. Manag. Sci. 21 (2), 47–61. http://dx.doi.org/10.1016/j.sorms.2016.12.001.
- Center for Research on the Epidemiology of Disasters (CRED), 2021. EM-DAT: The emergency events database. Number of natural disaster. Available at: https://public.emdat.be/.
- Chen, J., Lim, C.H., Qian, P.Z., Linderoth, J., Wright, S.J., 2014. Validating sample average approximation solutions with negatively dependent batches. arXiv:1404. 7208v2.
- Coffrin, C., Van Hentenryck, P., Bent, R., 2012. Last-mile restoration for multiple interdependent infrastructures. Proc. Natl. Conf. Artif. Intell. 26 (1), 455–463.
- CPLEX, IBM., 2021. CPLEX Optimizer | IBM. https://www.ibm.com/analytics/cplex-optimizer
- Danziger, M.M., Shekhtman, L.M., Bashan, A., Berezin, Y., Havlin, S., 2016. Vulner-ability of interdependent networks and networks of networks. In: Understanding Complex Systems. Springer International Publishing, Switzerland, pp. 79–99. http://dx.doi.org/10.1007/978-3-319-23947-7 5.
- de la Torre, L.E., Dolinskaya, I.S., Smilowitz, K.R., 2012. Disaster relief routing: Integrating research and practice. Socio-Econ. Plan. Sci. 46 (1), 88–97, Special Issue: Disaster Planning and Logistics: Part 1.
- Di Muro, M.A., La Rocca, C.E., Stanley, H.E., Havlin, S., Braunstein, L.A., 2016. Recovery of interdependent networks. Sci. Rep. 6 (22834), 1–11. http://dx.doi. org/10.1038/srep22834.
- Dupačová, J., Gröwe-Kuska, N., Römisch, W., 2003. Scenario reduction in stochastic programming. Math. Program. 95 (3), 493–511.
- Enayaty Ahangar, N., Sullivan, K.M., Nurre, S.G., 2020. Modeling interdependencies in infrastructure systems using multi-layered network flows. Comput. Oper. Res. 117, 104883. http://dx.doi.org/10.1016/j.cor.2019.104883.
- Escudero, L.F., Garín, M.A., Unzueta, A., 2017. Scenario cluster Lagrangean decomposition for risk averse in multistage stochastic optimization. Comput. Oper. Res. 85, 154–171, URL http://www.sciencedirect.com/science/article/pii/ S0305054817300989.
- Eusgeld, I., Nan, C., Dietz, S., 2011. "System-of-system" approach for interdependent critical infrastructures. Reliab. Eng. Syst. Saf. 96 (6), 679–686. http://dx.doi.org/ 10.1016/j.ress.2010.12.010.
- Fang, Y., Pedroni, N., Zio, E., 2016. Resilience-based component importance measures for critical infrastructure network systems. IEEE Trans. Reliab. 65 (2), 502–512. http://dx.doi.org/10.1109/tr.2016.2521761.
- Fang, Y., Sansavini, G., 2017. Emergence of antifragility by optimum postdisruption restoration planning of infrastructure networks. J. Infrastructure Syst. 23 (4), 04017024.
- Fang, Y., Sansavini, G., 2019. Optimum post-disruption restoration under uncertainty for enhancing critical infrastructure resilience. Reliab. Eng. Syst. Saf. 185 (January 2019), 1–11.
- Fares, R.L., King, C.W., 2017. Trends in transmission, distribution, and administration costs for U.S. investor-owned electric utilities. Energy Policy 105, 354–362. http: //dx.doi.org/10.1016/j.enpol.2017.02.036.
- Force, HurricaneSandyRebuildingTaskForce., 2013. Hurricane sandy rebuilding strategy. In: US Department of Housing and Urban Development., Washington, DC. Department of Housing and Urban Development,, Washington, DC.
- Franchin, P., Cavalieri, F., 2015. Probabilistic assessment of civil infrastructure resilience to earthquakes. Comput.-Aided Civ. Infrastruct. Eng. 30 (7), 583–600. http://dx.doi.org/10.1111/mice.12092.
- Garay-Sianca, A., Pinkley, S.G.N., 2021. Interdependent integrated network design and scheduling problems with movement of machines. European J. Oper. Res. 289 (1), 297–327.
- Ghorbani-Renani, N., González, A.D., Barker, K., Morshedlou, N., 2020. Protection-interdiction-restoration: Tri-level optimization for enhancing interdependent network resilience. Reliab. Eng. Syst. Saf. 199, 106907. http://dx.doi.org/10.1016/j.ress.2020.106907.

- Gong, J., Lee, E.E., Mitchell, J.E., Wallace, W.A., 2009. Logic-based MultiObjective optimization for restoration planning. In: Chaovalitwongse, E.W. (Ed.), Springer Optimization and Its Applications, Vol. 30. Springer US, Boston, MA, pp. 305–324. http://dx.doi.org/10.1007/978-0-387-88617-6\_11.
- González, A.D., nas Osorio, L.D., Sánchez-Silva, M., Medaglia, A.L., 2016. The inter-dependent network design problem for optimal infrastructure system restoration. Comput.-Aided Civ. Infrastruct. Eng. 31 (5), 334–350. http://dx.doi.org/10.1111/mice.12171.
- Guidotti, R., Chmielewski, H., Unnikrishnan, V., Gardoni, P., McAllister, T., van de Lindt, J., 2016. Modeling the resilience of critical infrastructure: the role of network dependencies. Sustain. Resilient Infrastructure 1 (3–4), 153–168. http: //dx.doi.org/10.1080/23789689.2016.1254999.
- Haimes, Y.Y., Jiang, P., 2001. Leontief-based model of risk in complex interconnected infrastructures. J. Infrastructure Syst. 7 (1), 1–12. http://dx.doi.org/10.1061/(asce) 1076-0342(2001)7:1(1).
- HDR, 2012. City of Raymore water storage and water supply study. Available at: https://www.raymore.com/home/showpublisheddocument?id=1176.
- Heitsch, H., Römisch, W., 2003. Scenario reduction algorithms in stochastic programming. Comput. Optim. Appl. 24 (2/3), 187–206.
- Helbing, D., 2013. Globally networked risks and how to respond. Nature 497 (7447), 51–59. http://dx.doi.org/10.1038/nature12047.
- Henry, D., Ramirez-Marquez, J.E., 2012. Generic metrics and quantitative approaches for system resilience as a function of time. Reliab. Eng. Syst. Saf. 99, 114–122.
- Holden, R., Val, D.V., Burkhard, R., Nodwell, S., 2013. A network flow model for interdependent infrastructures at the local scale. Saf. Sci. 53, 51–60. http://dx.doi. org/10.1016/j.ssci.2012.08.013.
- Horejšová, M., Vitali, S., Kopa, M., Moriggia, V., 2020. Evaluation of scenario reduction algorithms with nested distance. Comput. Manag. Sci. 17 (2), 241–275.
- Hosseini, S., Barker, K., Ramirez-Marquez, J.E., 2016. A review of definitions and measures of system resilience. Reliab. Eng. Syst. Saf. 145, 47–61.
- Humphreys, B.E., 2019. Critical Infrastructure: Emerging Trends and Policy Considerations for Congress. CRS Report No. R45809, Congressional Research Service, Washington, DC.
- Karagiannis, G.M., Chondrogiannis, S., Krausmann, E., Turksezer, Z.I., 2017. Power Grid Recovery After Natural Hazard Impact. Technical Report EUR 28844 EN, Publications Office of the European Union, Luxembourg, http://dx.doi.org/10. 2760/87402.
- Karakoc, D.B., Almoghathawi, Y., Barker, K., González, A.D., Mohebbi, S., 2019. Community resilience-driven restoration model for interdependent infrastructure networks. Int. J. Disaster Risk Reduct. 38, 101228. http://dx.doi.org/10.1016/j. ijdrr.2019.101228.
- Kim, Y., Spencer, B.F.J., Song, J., Elnashai, A.S., Stokes, T., 2007. Seismic performance assessment of interdependent lifeline systems. MAE Center Rep. CD Release 07-16.
- Kleywegt, A.J., Shapiro, A., Homem-de-Mello, T., 2002. The sample average approximation method for stochastic discrete optimization. SIAM J. Optim. 12 (2), 479-502
- Krokhmal, P., Palmquist, J., Uryasev, S., 2002. Portfolio optimization with conditional value-at-risk objective and constraints. J. Risk 4, 43–68.
- Laboratory, L.B.N., Nexant, I., 2021. The interruption cost estimate (ICE) calculator - lawrence berkeley national laboratory and nexant, inc. Available at: https://icecalculator.com/home.
- Lee I.I., E.E., Mitchell, J.E., Wallace, W.A., 2007. Restoration of services in interdependent infrastructure systems: A network flows approach. IEEE Trans. Syst. Man Cybern. C (Appl. Rev.) 37 (6), 1303–1317. http://dx.doi.org/10.1109/TSMCC.2007. 905859.
- Little, R.G., 2002. Controlling cascading failure: Understanding the vulnerabilities of interconnected infrastructures. J. Urban Technol. 9 (1), 109–123. http://dx.doi. org/10.1080/106307302317379855.
- Manuel, J., 2013. The long road to recovery: Environmental health impacts of hurricane sandy. Environ. Health Perspect. 121 (5).
- Meltzer, A., Beck, S., Ruiz, M., Hoskins, M., Soto-Cordero, L., Stachnik, J.C., Lynner, C., Porritt, R., Portner, D., Alvarado, A., Hernandez, S., Yepes, H., Charvis, P., Font, Y., Regnier, M., Agurto-Detzel, H., Rietbrock, A., Leon-Rios, S., Mercerat, E.D., 2019. The 2016 Mw 7.8 pedernales, ecuador, earthquake: Rapid response deployment. Seismol. Res. Lett. 90 (3), 1346–1354. http://dx.doi.org/10.1785/0220180364.
- Memphis Light, Gas, Water Division (MLGW), 2021. Facts & figures 2017. Available at: http://www.mlgw.com/images/content/files/pdf/FactsFigures2018.pdf.
- Mendonca, D., Lee, E., Wallace, W., 2004. Impact of the 2001 world trade center attack on critical interdependent infrastructures. In: 2004 IEEE International Conference on Systems, Man and Cybernetics (IEEE Cat. No.04CH37583), Vol. 5. IEEE, http: //dx.doi.org/10.1109/icsmc.2004.1401165.
- Mete, H.O., Zabinsky, Z.B., 2010. Stochastic optimization of medical supply location and distribution in disaster management. Int. J. Prod. Econ. 126 (1), 76–84. http://dx.doi.org/10.1016/j.ijpe.2009.10.004, Improving Disaster Supply Chain Management Key supply chain factors for humanitarian relief.
- Min, H.-S.J., Beyeler, W., Brown, T., Son, Y.J., Jones, A.T., 2007. Toward modeling and simulation of critical national infrastructure interdependencies. IIE Trans. 39 (1), 57–71. http://dx.doi.org/10.1080/07408170600940005.
- Mooney, E.L., Almoghathawi, Y., Barker, K., 2019. Facility location for recovering systems of interdependent networks. IEEE Syst. J. 13 (1), 489–499. http://dx.doi. org/10.1109/jsyst.2018.2869391.

- Morales, J.M., Pineda, S., Conejo, A.J., Carrión, M., 2009. Scenario reduction for futures market trading in electricity markets. IEEE Trans. Power Syst. 24 (2), 878–888.
- Moreno, A., Munari, P., Alem, D., 2019. A branch-and-benders-cut algorithm for the crew scheduling and routing problem in road restoration. European J. Oper. Res. 275 (1), 16–34. http://dx.doi.org/10.1016/j.ejor.2018.11.004.
- Morshedlou, N., González, A.D., Barker, K., 2018. Work crew routing problem for infrastructure network restoration. Transp. Res. B 118, 66–89. http://dx.doi.org/ 10.1016/j.trb.2018.10.001.
- Noyan, N., 2012. Risk-averse two-stage stochastic programming with an application to disaster management. Comput. Oper. Res. 39 (3), 541–559. http://dx.doi.org/10. 1016/j.cor.2011.03.017.
- Nurre, S.G., Cavdaroglu, B., Mitchell, J.E., Sharkey, T.C., Wallace, W.A., 2012. Restoring infrastructure systems: An integrated network design and scheduling (INDS) problem. European J. Oper. Res. 223 (3), 794–806.
- Nurre, S.G., Sharkey, T.C., 2014. Integrated network design and scheduling problems with parallel identical machines: Complexity results and dispatching rules. Networks 63 (4), 306–326.
- Ouyang, M., 2014. Review on modeling and simulation of interdependent critical infrastructure systems. Reliab. Eng. Syst. Saf. 121, 43–60. http://dx.doi.org/10. 1016/j.ress.2013.06.040.
- Ouyang, M., Wang, Z., 2015. Resilience assessment of interdependent infrastructure systems: With a focus on joint restoration modeling and analysis. Reliab. Eng. Syst. Saf. 141, 74–82. http://dx.doi.org/10.1016/j.ress.2015.03.011.
- Peerenboom, J., Fisher, R., Rinaldi, S., Kelly, T., 2002. Studying the chain reaction. Electr. Perspect. 27 (1), 22–35.
- Executive Office of the President, CouncilofEconomicAdvisers., 2013. Economic Benefits of Increasing Electric Grid Resilience to Weather Outages. The Council, Washington, D.C..
- Python, 2021. Python.org. https://www.python.org/.
- Rachev, S.T., 1991. Probability Metrics and the Stability of Stochastic Models, Scenario. Wiley, Chichester New York.
- Rahmaniani, R., Crainic, T.G., Gendreau, M., Rei, W., 2017. The benders decomposition algorithm: A literature review. European J. Oper. Res. 259 (3), 801–817. http://dx.doi.org/10.1016/j.eior.2016.12.005.
- Rinaldi, S.M., 2004. Modeling and simulating critical infrastructures and their interdependencies. In: 37th Annual Hawaii International Conference on System Sciences, 2004. Proceedings of the. IEEE, pp. 5–8. http://dx.doi.org/10.1109/hicss.2004. 1265180
- Rinaldi, S.M., Peerenboom, J.P., Kelly, T.K., 2001. Identifying, understanding, and analyzing critical infrastructure interdependencies. IEEE Control Syst. 21 (6), 11–25. http://dx.doi.org/10.1109/37.969131.
- Rockafellar, R.T., Uryasev, S., 2000. Optimization of conditional value-at-risk. J. Risk 2 (3), 21–41.

- Saidi, S., Kattan, L., Jayasinghe, P., Hettiaratchi, P., Taron, J., 2018. Integrated infrastructure systems–A review. Sustainable Cities Soc. 36, 1–11. http://dx.doi. org/10.1016/j.scs.2017.09.022.
- Sharkey, T.C., Cavdaroglu, B., Nguyen, H., Holman, J., Mitchell, J.E., Wallace, W.A., 2015. Interdependent network restoration: On the value of information-sharing. European J. Oper. Res. 244 (1), 309–321.
- Sharma, N., Tabandeh, A., Gardoni, P., 2017. Resilience analysis: A mathematical formulation to model resilience of engineering systems. Sustain. Resilient Infrastructure 3 (2), 49–67. http://dx.doi.org/10.1080/23789689.2017.1345257.
- Tootaghaj, D.Z., Bartolini, N., Khamfroush, H., Porta, T.L., 2017. Controlling cascading failures in interdependent networks under incomplete knowledge. In: 2017 IEEE 36th Symposium on Reliable Distributed Systems (SRDS). IEEE, Hong Kong, http://dx.doi.org/10.1109/srds.2017.14.
- Unsihuay, C., Lima, J.W.M., de Souza, A.Z., 2007. Modeling the integrated natural gas and electricity optimal power flow. In: 2007 IEEE Power Engineering Society General Meeting. IEEE, Tampa, FL, pp. 24–28. http://dx.doi.org/10.1109/pes.2007. 386124.
- Vugrin, E.D., Turnquist, M.A., Brown, N.J., 2014. Optimal recovery sequencing for enhanced resilience and service restoration in transportation networks. Int. J. Crit. Infrastruct. 10 (3/4), 218–246.
- Wallace, W., Mendonca, D., Lee, E., Mitchell, J., Wallace, J., Monday, J., 2003.
  Managing disruptions to critical interdependent infrastructures in the context of the 2001 world trade center attack. In beyond september 11th: An account of. Post-Disaster Res., Special Publ. 39, 165–198.
- White House, 2013. Presidential Policy Directive/PPD-21: Critical Infrastructure Security and Resilience. Office of the Press Secretary: Washington, DC.. Office of the Press Secretary, Washington, DC..
- Wolfram, C., 2021. Measuring the economic costs of the PG&E outages. Available at: https://energyathaas.wordpress.com/2019/10/14/measuring-the-economic-costs-of-the-pge-outages/.
- Wyss, G.D., Jorgensen, K.H., 1998. A user 's guide to LHS: Sandia's latin hypercube sampling software acknowledgments. Distribution (February), 88.
- Zhang, C., Kong, J.-j., Simonovic, S.P., 2018. Restoration resource allocation model for enhancing resilience of interdependent infrastructure systems. Saf. Sci. 102, 169–177. http://dx.doi.org/10.1016/j.ssci.2017.10.014.
- Zhang, P., Peeta, S., 2011. A generalized modeling framework to analyze interdependencies among infrastructure systems. Transp. Res. B 45 (3), 553–579. http://dx.doi.org/10.1016/j.trb.2010.10.001.
- Zhang, Y., Yang, N., Lall, U., 2016. Modeling and simulation of the vulnerability of interdependent power-water infrastructure networks to cascading failures. J. Syst. Sci. Syst. Eng. 25 (1), 102–118. http://dx.doi.org/10.1007/s11518-016-5295-3.
- Zimmerman, R., 2001. Social implications of infrastructure network interactions. J. Urban Technol. 8 (3), 97–119. http://dx.doi.org/10.1080/106307301753430764.